



저작자표시-비영리-변경금지 2.0 대한민국

이용자는 아래의 조건을 따르는 경우에 한하여 자유롭게

- 이 저작물을 복제, 배포, 전송, 전시, 공연 및 방송할 수 있습니다.

다음과 같은 조건을 따라야 합니다:



저작자표시. 귀하는 원저작자를 표시하여야 합니다.



비영리. 귀하는 이 저작물을 영리 목적으로 이용할 수 없습니다.



변경금지. 귀하는 이 저작물을 개작, 변형 또는 가공할 수 없습니다.

- 귀하는, 이 저작물의 재이용이나 배포의 경우, 이 저작물에 적용된 이용허락조건을 명확하게 나타내어야 합니다.
- 저작권자로부터 별도의 허가를 받으면 이러한 조건들은 적용되지 않습니다.

저작권법에 따른 이용자의 권리는 위의 내용에 의하여 영향을 받지 않습니다.

이것은 [이용허락규약\(Legal Code\)](#)을 이해하기 쉽게 요약한 것입니다.

[Disclaimer](#)

Thesis for the Degree of Master of Engineering

**1-D basin modeling of the Kunsan Basin,
Yellow Sea and implications**



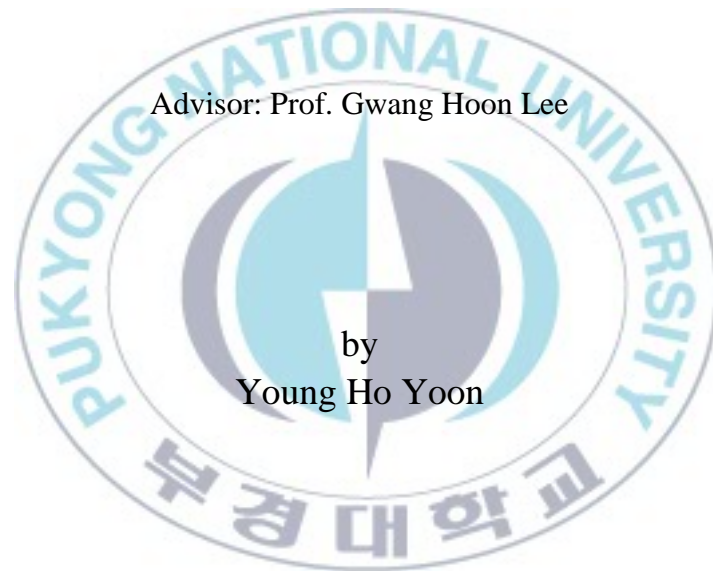
by
Young Ho Yoon

Department of Environmental Exploration Engineering
The Graduate School

Pukyong National University
February 2010

1-D basin modeling of the Kunsan Basin, Yellow Sea and implications

(황해 군산분지의 1 차원
분지모델링 연구)



A thesis submitted in partial fulfillment of the requirements
for the degree of

Master of Engineering

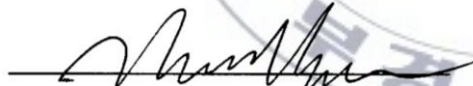
in Department of Environmental Exploration Engineering,
The Graduate School,
Pukyong National University
February 2010

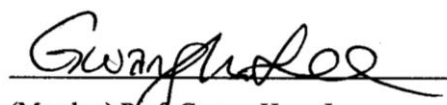
1-D basin modeling of the Kunsan Basin,
Yellow Sea and implications

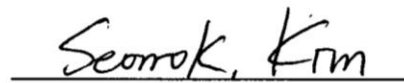
A thesis
by
Young Ho Yoon



Approved by:


(Chairman) Prof. Dae Choul Kim


(Member) Prof. Gwang Hoon Lee


(Member) Prof. Seon-Ok Kim

February 2010

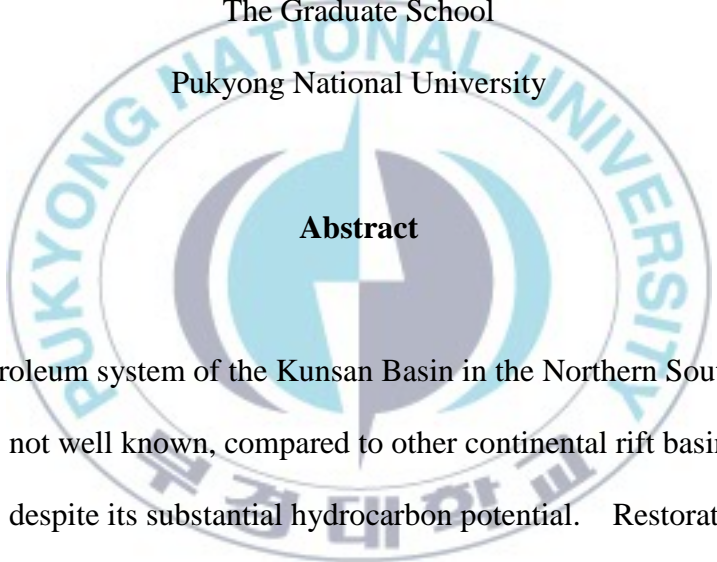
1-D basin modeling of the Kunsan Basin, Yellow Sea and implications

Young Ho Yoon

Department of Environmental Exploration Engineering

The Graduate School

Pukyong National University

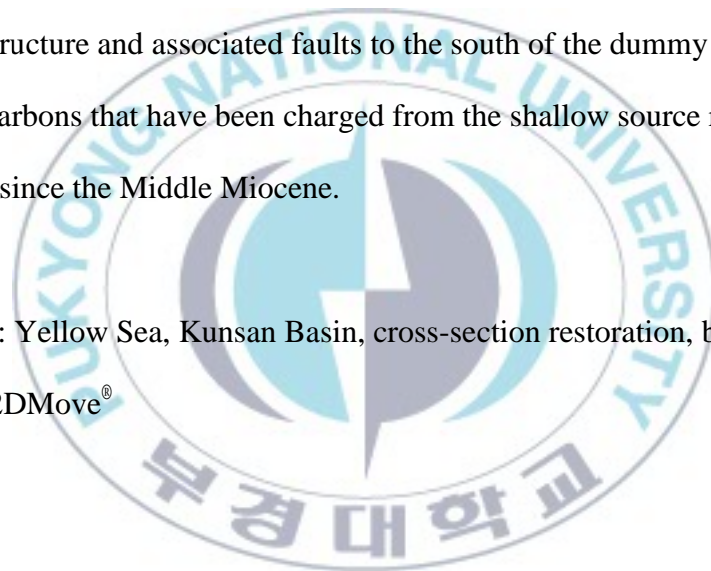


Abstract

The petroleum system of the Kunsan Basin in the Northern South Yellow Sea Basin is not well known, compared to other continental rift basins in the Yellow Sea, despite its substantial hydrocarbon potential. Restoration of two depth-converted seismic profiles across the Central Subbasin in the southern Kunsan Basin shows that extension was interrupted by inversions in the Late Oligocene-Middle Miocene that created anticlinal structures. One-dimensional basin modeling of the IIH-1Xa well suggests that hydrocarbon expulsion in the northeastern margin of the depocenter of the Central Subbasin peaked in the Early Oligocene, predating the inversions. Hydrocarbon generation at the dummy well location in the depocenter of the subbasin began

in the Late Paleocene. Most source rocks in the depocenter passed the main expulsion phase except for the shallowest source rocks. Hydrocarbons generated from the depocenter are likely to have migrated southward toward the anticlinal structure and faults away from the traps along the northern and northeastern margins of the depocenter because the basin-fill strata are dipping north. Faulting that continued during the rift phase (~ Middle Miocene) of the subbasin probably acted as conduits for the escape of hydrocarbons. Thus, the anticlinal structure and associated faults to the south of the dummy well may trap hydrocarbons that have been charged from the shallow source rocks in the depocenter since the Middle Miocene.

Key words: Yellow Sea, Kunsan Basin, cross-section restoration, basin modeling, 2DMove[®]



황해 군산분지의 1 차원 분지모델링 연구

윤영호

부경대학교 대학원 에너지자원공학과

요약

남황해분지내의 군산분지는 탄화수소의 부존 가능성이 매우 높음에도 불구하고 황해의 다른 분지들과 비교해서 상대적으로 탄화수소와 관련된 연구가 충분히 이루어지지 않았다. 군산분지의 퇴적 깊이가 최대인 지역을 가로지르는 두 탄성과 측선을 깊이 단면으로 변환한 후에 2DMove[®]로 구조복원하여, 백악기 후기 이후로 침강을 시작하였으며, 후기 올리고세와 중기 마이오세 사이에 구조역전에 의해 배사구조들을 형성했다는 것을 확인하였다.

분지의 북동쪽 주변부에 위치하는 IIIH-1Xa 시추공의 1차원 분지 모델링은 깊은 근원암에서 초기 에오세에 탄화수소 생성이 시작되었으며 초기 올리고세에 탄화수소의 배출이 최대였음을 보여준다. IIIH-1Xa 시추공 지역 천부의 근원암은 열적으로 성숙되지 않았다. 퇴적된 층이 가장 두꺼운 지역에 위치하는 가상 시추공에서는 탄화수소의 생성이 후기 팔레오세에 시작되었으며 현재도 계속되고 있다. 가상 시추공 지역에서의 탄화수소 배출은 초기 에오세에 시작하여 현재까지 진행되고 있다. 그러나 가상 시추공 지역에서 형성된 탄화수소는 분지 지층들이

북쪽 방향으로 회전되어 경사를 이루고 있기 때문에 분지의 북동 주변부의 트랩으로부터 멀어지며 남쪽의 배사구조를 향하여 이동했을 것으로 보여진다. 연구 지역에 분포하는 단층들은 적어도 중기 마이오세까지 활동하였으며 탄화수소의 트랩을 형성하였을 뿐 아니라 탄화수소의 누출경로 역할도 했을 것으로 생각된다.

색인어: 황해, 군산분지, 축선복원, 분지모델링, 2DMove[®]



Table of Contents

Abstract	i
Abstract (In Korean)	iii
Table of Contents	v
List of Figures	vii
List of Tables	xii
1. INTRODUCTION	1
2. GEOLOGIC SETTING	5
3. CROSS-SECTION RESTORATION	9
3.1. Methods	9
3.2. Results and interpretation	16
3.2.1 Line 1	16
3.2.2 Line 2	20
4. BASIN MODELING	24
4.1. Methods	24
4.2. Results and interpretation	31
5. DISCUSSION	38
6. SUMMARY AND CONCLUSIONS	43
7. ACKNOWLEDGEMENTS	45



List of Figures

- Figure 1.** Bathymetry of the Yellow Sea and vicinity and major Cenozoic basins, modified from Lee et al. (2006). Basin locations are adapted from Liu (1986), Zhang et al. (1989), and Yi et al. (2003). Inset is the tectonic map of eastern China and the Yellow Sea from Kim et al. (2000). Contour interval is in meters. ----- 2
- Figure 2.** Bathymetry of the Kunsan Basin and locations of exploratory wells. Heavy lines indicate seismic profiles and their depth-converted sections restored in this study. Dummy well is located at the intersection of these seismic profiles. Contour interval is in meters. ----- 4
- Figure 3.** Depth-structure map of the top of the acoustic basement modified from Han (2008). The depths of the acoustic basement range from less than 400 m over basement highs to more than 8,000 m in the southwestern part of the Central Subbasin. Large basement faults form the boundaries of the subbasins. Contour interval is in meters. ----- 7
- Figure 4.** Line 1. The curved downward-flattening basement fault in the southwest forms the southern boundary of the Central Subbasin. The large SW-dipping fault soles out into this fault. Rotation of the SW-dipping fault resulted in thicker sediment accumulation (S4 – S6) in the hanging wall. The dummy well is located in the depocenter of the Central Subbasin. Ages of the unconformities including the top of the acoustic basement were estimated from the correlation at the IIIH-1Xa well with the unconformities reported by

KIGAM (1997) and Ryu et al. (2000). See Fig. 2 for location. ----- 10

Figure 5. Line 2. The curved downward-flattening basement fault in the southeast forms the southern boundary of the Central Subbasin. The SW- and smaller S-dipping faults (see Fig. 3 for fault orientation) sole out into this fault. Rotation of the SW- and S-dipping faults resulted in thicker sediment accumulation (S3 – S5) in the hanging wall. The dummy well is located in the depocenter of the subbasin. Ages of the unconformities including the top of the acoustic basement were estimated from the correlation at the IIH-1Xa well with the unconformities reported by KIGAM (1997) and Ryu et al. (2000). See Fig. 2 for location. ----- 11

Figure 6. Age control at the IIH-1Xa well from (A) KIGAM (1997) and (B) Ryu et al. (2000). (C) Seismic sequences identified in this study and the ages of their boundaries. The sequence boundaries or unconformity surfaces were correlated at the IIH-1Xa well with those of KIGAM (1997) and Ryu et al. (2000). Ages of the unconformity surfaces were estimated, assuming that the sediment accumulation rates between the key unconformity surfaces were constant. ----- 12

Figure 7. Cross-section restoration procedure. The depth models for Lines 1 and 2 were constructed from seismic profiles using Kingdom Suite[®]. 2DMove[®] was used for cross-section restoration. ----- 14

Figure 8. Sequential restoration of the depth model of Line 1. Vertical exaggeration is approximately 2×. ----- 17

Figure 9. Sequential restoration of the depth model of Line 2. Vertical exaggeration is approximately 2×. ----- 21

Figure 10. (A) Seismic facies interpreted as lacustrine sediments is characterized by moderate- to high-amplitude, continuous reflections, onlapping onto the underlying layer. (B) Seismic facies interpreted as nonmarine/fluvial sediments is characterized by variable amplitude reflections with poor continuity. ----- 26

Figure 11. (A) Stratigraphic column, thicknesses of ten sequences, and source rock locations of the dummy well. (B) Stratigraphic column, thicknesses of ten sequences, and source rock locations of the IHH-1Xa well. The IHH-1Xa well was extended beyond the actual bottom depth (3,467 m) to the basement (4,365 m) to include the deep source rocks in basin modeling. ----- 27

Figure 12. (A) Burial history and hydrocarbon windows; (B) burial history and expulsion windows; and (C) expelled hydrocarbons per time interval for the dummy well. Oil generation began in the Late Paleocene from the deep source rocks and in the Late Oligocene from the shallow source rocks. Most source rocks passed the main expulsion phase except for the shallowest source rock (source #6). The volumes of hydrocarbons expelled from the nonmarine/fluvial source rocks (source rocks # 2, 4) were very small. ----- 32

Figure 13. (A) Burial history and hydrocarbon windows; (B) burial history and expulsion windows; and (C) expelled hydrocarbons per time interval for the IHH-1Xa well. Hydrocarbon expulsion from the deep source rocks began

in the Middle Eocene and peaked in the Early Oligocene. Only very small amounts of hydrocarbons are currently being expelled from the deep source rocks. ----- 35

Figure 14. Petroleum event chart for the Central Subbasin. The inversions largely postdated the main phase of hydrocarbon expulsion in the northeastern margin of the depocenter of the subbasin but predated the hydrocarbon expulsion from the shallow source rocks in the depocenter of the subbasin.

Faults remained active until the Middle Miocene. ----- 39

Figure 15. (A) Schematic cross-sectional diagram showing hydrocarbon migration for Oligocene-Middle Miocene time. Hydrocarbons from the depocenter of the Central Subbasin migrated preferentially toward the anticlinal structure and faults in the south. However, most of these hydrocarbons leaked through the faults during the rift phase of the subbasin (~ Middle Miocene) when faulting remained active. Hydrocarbons from the deep parts of the subbasin to the north of the large SW-dipping fault migrated northward but were probably intercepted by the fault immediately south of the anticline penetrated by the IHH-1Xa well. (B) Schematic cross-sectional diagram showing hydrocarbon migration for the present day. Cessation of faulting sometime in the Middle Miocene had significant impact on the trapping potential. Hydrocarbons from the shallow source rocks in the deepest part of the subbasin have migrated southward and may be filling the anticlinal structure and associated fault traps to the south of the dummy well. Hydrocarbons from

the thick sediment fill to the north of the large SW-dipping fault probably have migrated northward and may be accumulating against the fault south of the IHH-1Xa well. ----- 41



List of Tables

Table 1. The key input parameters for one-dimensional basin modeling. ---- 29



1. Introduction

The Yellow Sea (Fig. 1) consists of Mesozoic-Cenozoic continental rift basins including the Bohai Bay, North Yellow Sea, Northern South Yellow Sea, and Jiangsu (Subei)-Southern South Yellow Sea basins. The Bohai Bay Basin is the most petroliferous basin in China, providing about one third of the total oil production of the country (Hao et al., 2009). In the Subei Basin, oil has been produced from a number of small fault blocks with multiple reservoirs (Liu et al., 2007). Small volumes of oil have been produced in the West Korea Bay Basin in the eastern North Yellow Sea Basin (Massoud et al., 1993; Wu et al., 2008). No commercial discovery has yet been made in the Northern South Yellow Sea Basin. Five wells were drilled in the Kunsan Basin in the eastern Northern South Yellow Sea Basin. These wells encountered shaly, poorly sorted sands and volcanoclastics (Shin, 2005). By 2004, a total of 33,800 km of 2-D multi-channel seismic data had been acquired from the Kunsan Basin (Shin, 2005). However, despite the extensive 2-D seismic surveys and exploratory drilling efforts, the petroleum system of the Kunsan Basin remains poorly understood. Timings of hydrocarbon generation and trap formation are not well constrained.

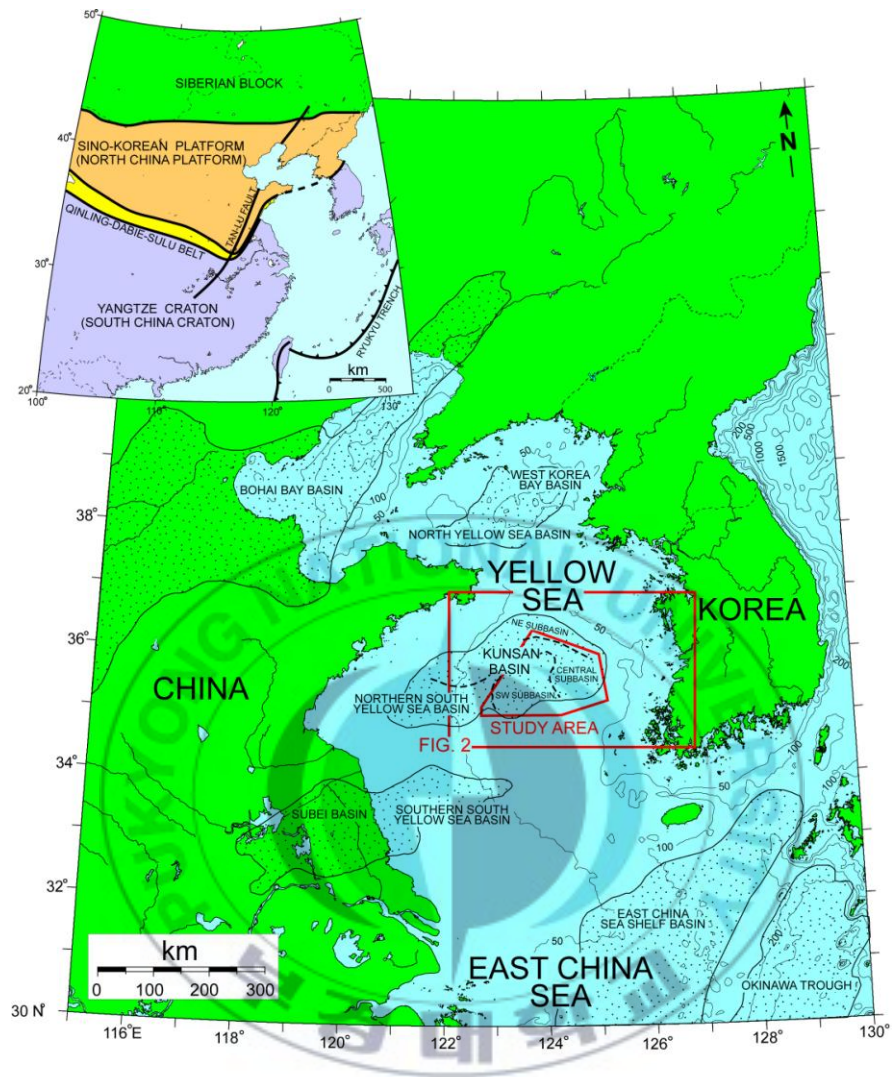
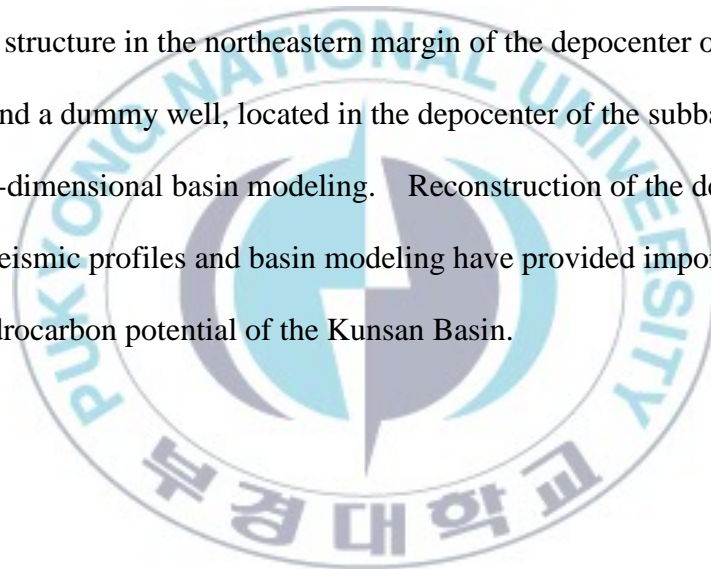


Fig. 1. Bathymetry of the Yellow Sea and vicinity and major Cenozoic basins, modified from Lee et al. (2006). Basin locations are adapted from Liu (1986), Zhang et al. (1989), and Yi et al. (2003). Inset is the tectonic map of eastern China and the Yellow Sea from Kim et al. (2000). Contour interval is in meters.

In this study, we sequentially restored two depth-converted seismic profiles traversing the depocenter of the Central Subbasin (Fig. 2) in the southern Kunsan Basin to investigate the timing of trap formation and to backtrack the subsidence history that was the key input parameter for one-dimensional basin modeling. The two seismic profiles were selected from a large data set, consisting of different vintages of 2-D multi-channel seismic profiles, acquired by various oil and service companies between 1986 and 2001. IIH-1Xa well, drilled on a structure in the northeastern margin of the depocenter of the Central Subbasin, and a dummy well, located in the depocenter of the subbasin, were used in one-dimensional basin modeling. Reconstruction of the depth-converted seismic profiles and basin modeling have provided important insights into the hydrocarbon potential of the Kunsan Basin.



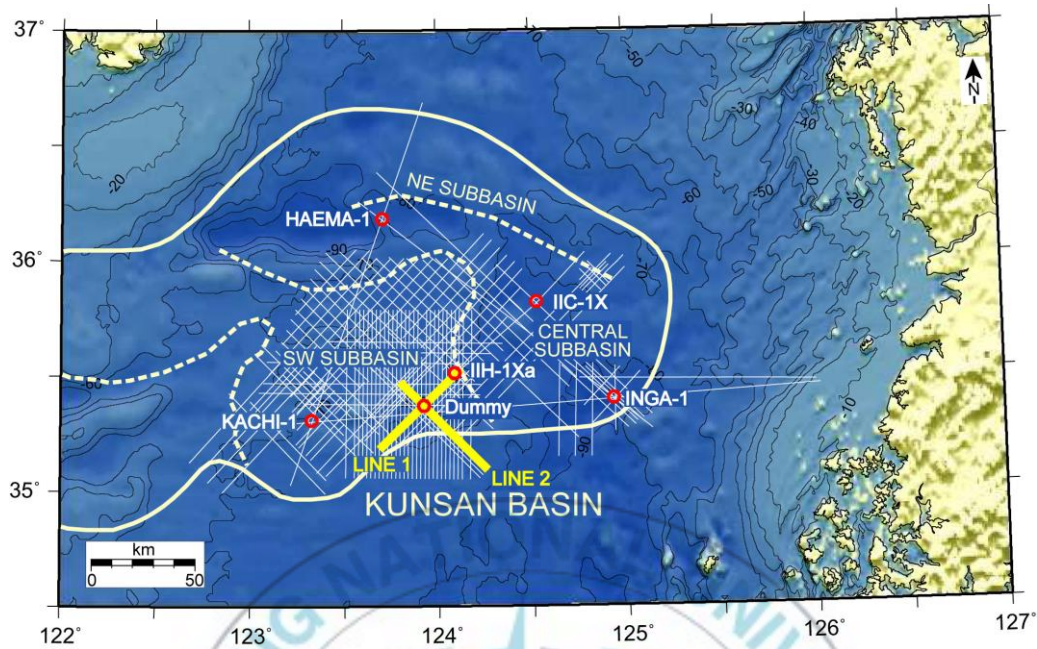


Fig. 2. Bathymetry of the Kunsan Basin and locations of exploratory wells. Heavy lines indicate seismic profiles and their depth-converted sections restored in this study. Dummy well is located at the intersection of these seismic profiles. Contour interval is in meters.

2. Geologic setting

The Yellow Sea (Fig. 1) is a very shallow (< 90 m), semi-enclosed continental shelf basin, lying between China and Korea. It can be divided into the northern and southern parts by the Qinling-Dabie-Sulu collisional belt (Kim et al., 2000; Wu, 2002). The Qinling-Dabie-Sulu collisional belt forms the suture zone where the northward moving Yangtze craton was accreted to the Sino-Korean platform in the Paleozoic-early Mesozoic (Hsü, 1989; Gilder and Courtillot, 1997). The northern Yellow Sea, including the Bohai Bay and North Yellow Sea Basin, and the southern Yellow Sea, including the Northern and Southern South Yellow Sea basins, belong to the Sino-Korean (or North China) platform and the Yangtze (or South China) craton, respectively (Ree et al., 1996; Kim et al., 2000).

In the early Mesozoic, the eastern margin of the sutured continent became an active zone of subduction (Hsü, 1989), which caused crustal extension toward the interior of the continent, creating numerous rift basins (Liu, 1986). The outer edge of the continent was also disintegrated, resulting in back-arc basins (e.g., the Philippine, Banda, Sulu seas) (Lee and McCabe, 1986). The disintegration processes continued throughout the Cenozoic and formed the Yellow Sea, East Sea (Japan Sea), East China Sea, and South China Sea (Hsü, 1989). The collision of India and Eurasia in the Middle to Late Eocene further

complicated the area, creating complex strike-slip faults (Tapponnier et al., 1982). During the Cenozoic, volcanism in association with extensional or transtensional faults was widespread across eastern China (Barry and Kent, 1998) and the Yellow Sea (Lee et al., 2006).

The rift basin development phase (Liu, 1986; Li, 1995) of the Yellow Sea consisted of rifting/downfaulting followed by subsidence/downwarping (Zhang et al., 1989). The development of the Northern South Yellow Sea Basin can be divided into six stages (Yi et al., 2003): (1) initial rifting during the Late Jurassic (?) – Cretaceous; (2) subsidence from the Paleocene to Middle Eocene; (3) alternation of uplift and subsidence in the Late Eocene; (4) synrift inversion and erosion throughout the Oligocene; (5) uplift during the Early Miocene; and (6) regional subsidence from the Middle Miocene onwards, interrupted briefly by uplift in the Early Pliocene. The basin fill of the Northern South Yellow Sea Basin is over 7,000-m thick and consists largely of nonmarine (fluvial-alluvial and lacustrine) sediments (Yi et al., 2003). Basement highs and faults divide the Northern South Yellow Sea Basin further into subbasins.

The Kunsan Basin in the eastern Northern South Yellow Sea Basin includes the southeastern part of the NE Subbasin and the eastern parts of the Central and SW subbasins (Figs. 1, 2, 3). The basin fill of the Kunsan Basin consists

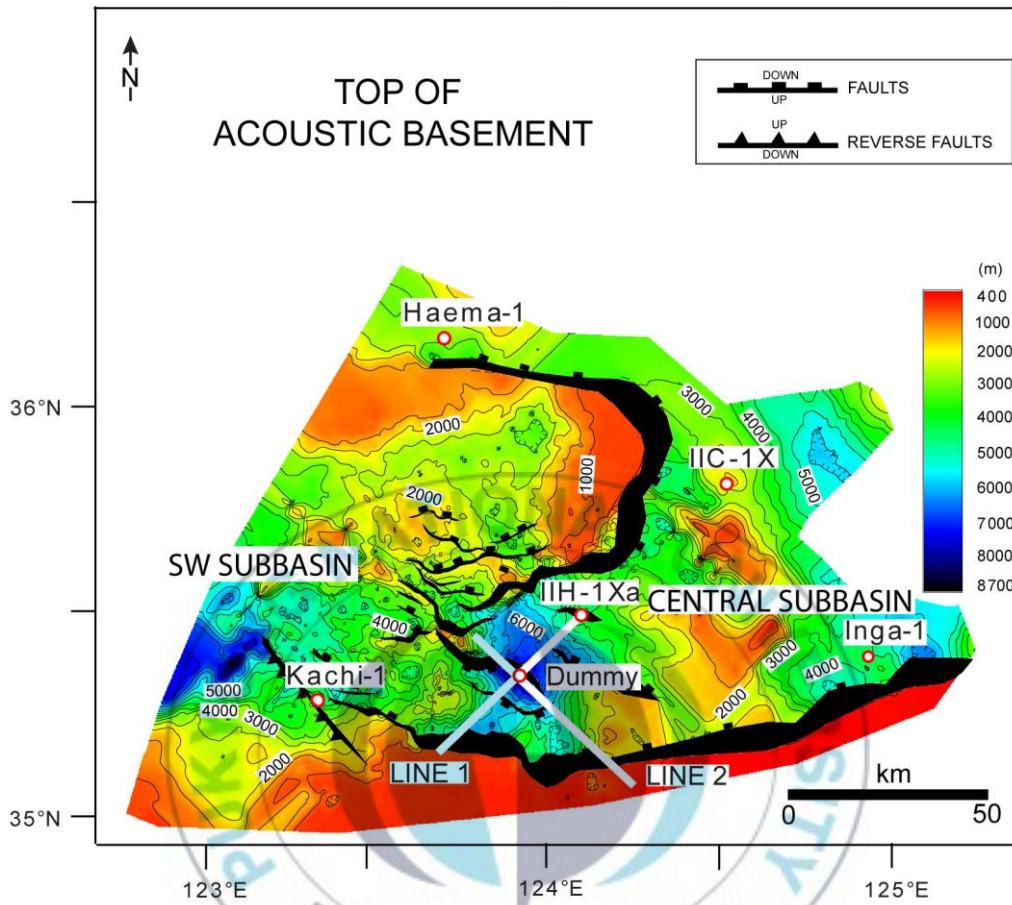


Fig. 3. Depth-structure map of the top of the acoustic basement modified from Han (2008). The depths of the acoustic basement range from less than 400 m over basement highs to more than 8,000 m in the southwestern part of the Central Subbasin. Large basement faults form the boundaries of the subbasins. Contour interval is in meters.

mainly of non-marine clastic sediments (Yi et al., 2003) and can be divided into three distinct tectono-stratigraphic units: pre-Cretaceous, Cretaceous-early Tertiary (Paleocene), and Tertiary (Eocene-present) (Shin, 2005). The Late Cretaceous and Paleocene shales are potential source rocks and the younger Paleocene-Eocene fluivio-deltaic sediments may form reservoirs (Shin, 2005).



3. Cross-section restoration

3.1 Methods

Two representative seismic profiles (Lines 1, 2; Figs. 4, 5), traversing the thickest part or depocenter of the Central Subbasin, were selected for cross-section restoration. The eight key unconformity surfaces and the top of the acoustic basement, identified and mapped originally by Han (2008), and one additional unconformity were correlated at the IIH-1Xa well with those of KIGAM (1997) and Ryu et al. (2000) (Fig. 6). The ages of these unconformities were estimated, assuming that the sediment accumulation rates between the key unconformity surfaces were constant. The sedimentary sequences bounded by the unconformities are referred to as S1 to S10 from oldest to youngest.

Acoustic and density logs from four exploratory wells (IIH-1Xa, IIC-1X, Haema-1, and Inga-1) were used to generate synthetic seismograms for synthetic-to-well tie that helped obtain the time-depth relationships at the well locations. The velocity field of the area was constructed from these time-depth relationships and used for time-depth conversion of the two seismic profiles. Kingdom Suite[®] (version 8.3) was used for synthetic-to-well tie and

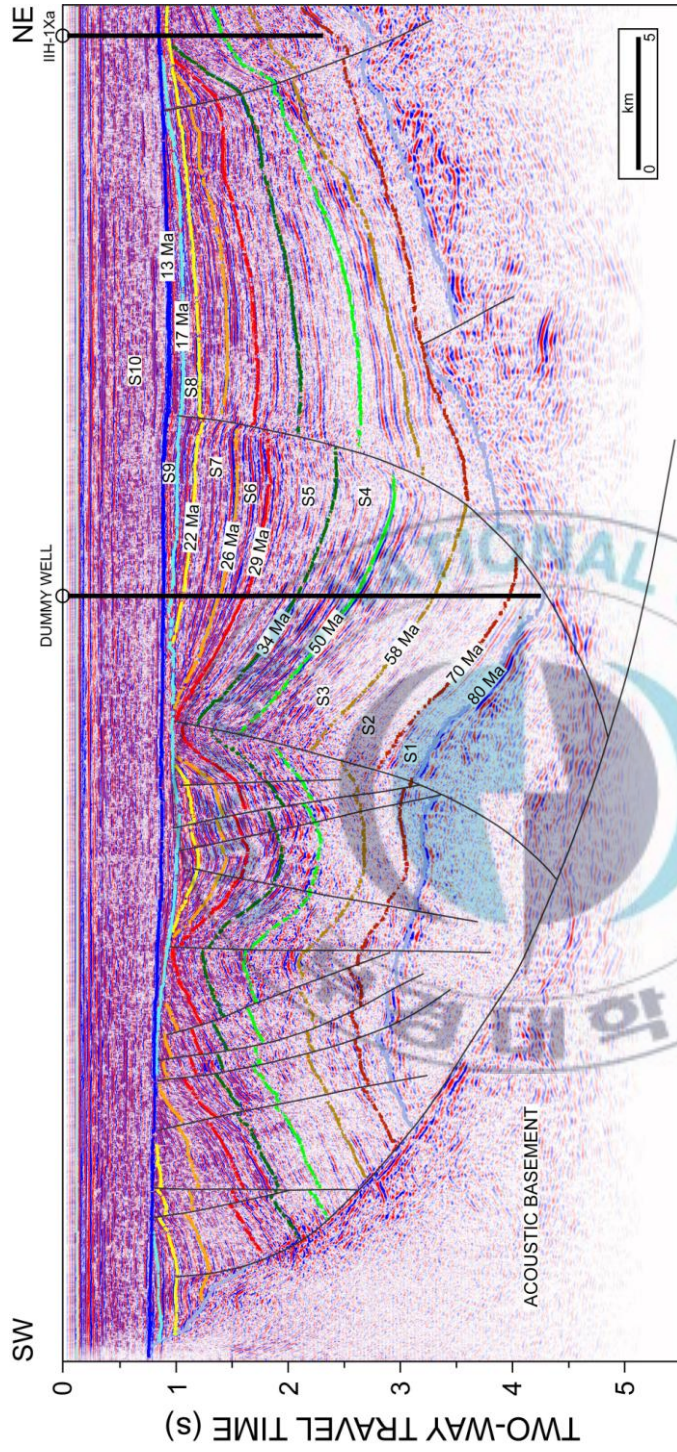


Fig. 4. Line 1. The curved downward-flattening basement fault in the southwest forms the southern boundary of the Central Subbasin. The large SW-dipping fault soles out into this fault. Rotation of the SW-dipping fault resulted in thicker sediment accumulation (S4 – S6) in the hanging wall. The dummy well is located in the depocenter of the Central Subbasin. Ages of the unconformities including the top of the acoustic basement were estimated from the correlation at the IIIH-1Xa well with the unconformities reported by KIGAM (1997) and Ryu et al. (2000). See Fig. 2 for location.

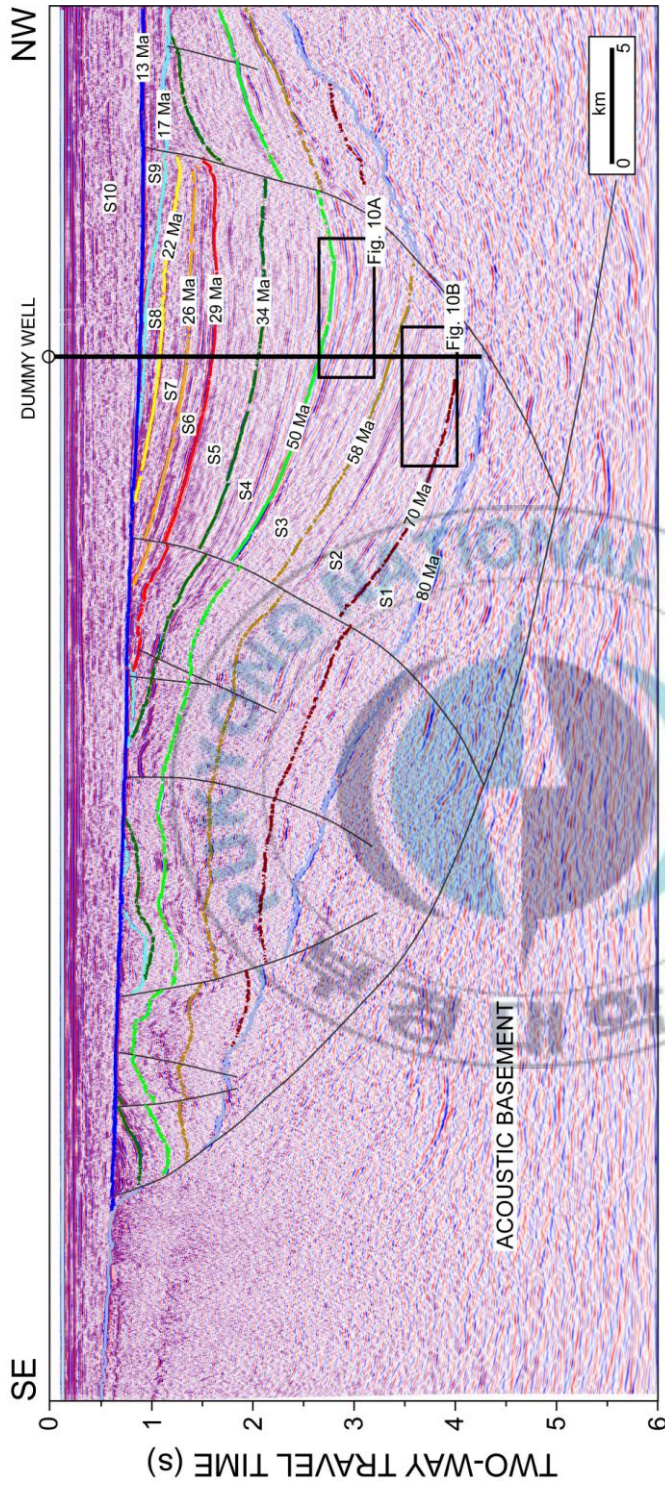


Fig. 5. Line 2. The curved downward-flattening basement fault in the southeast forms the southern boundary of the Central Subbasin. The SW- and smaller S-dipping faults (see Fig. 3 for fault orientation) sole out into this fault. Rotation of the SW- and S-dipping faults resulted in thicker sediment accumulation (S3 – S5) in the hanging wall. The dummy well is located in the depocenter of the subbasin. Ages of the unconformities including the top of the acoustic basement were estimated from the correlation at the IHH-1Xa well with the unconformities reported by KIGAM (1997) and Ryu et al. (2000). See Fig. 2 for location.

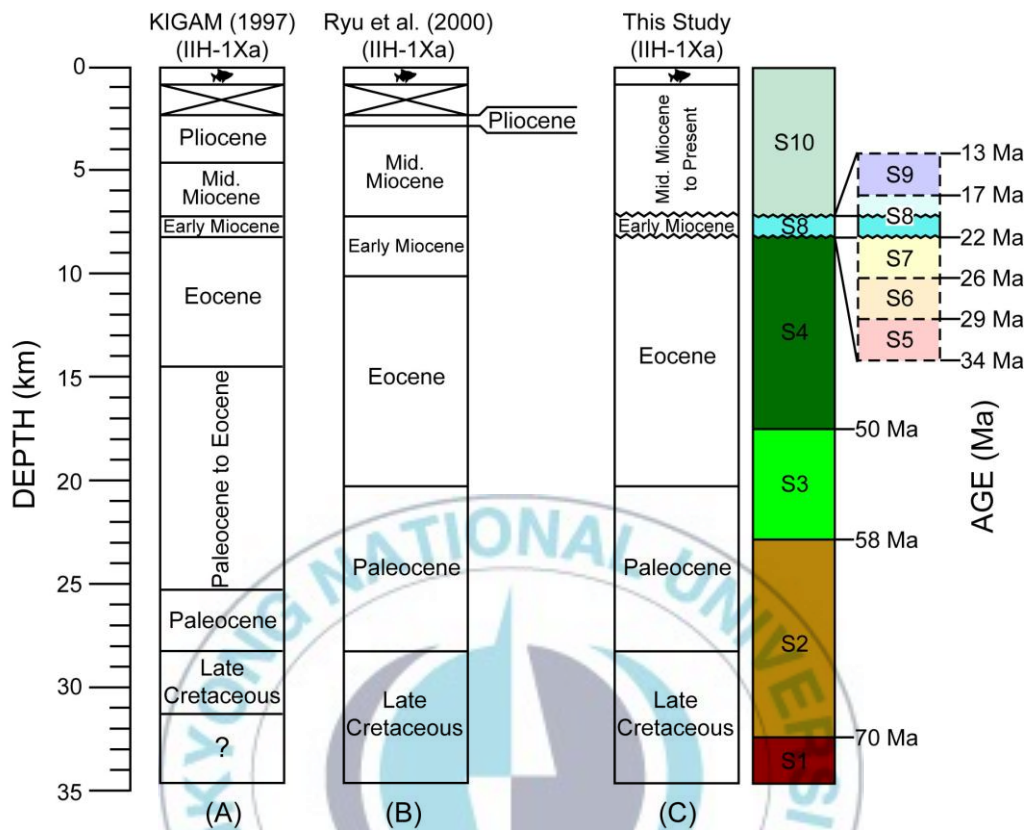


Fig. 6. Age control at the IIH-1Xa well from (A) KIGAM (1997) and (B) Ryu et al. (2000). (C) Seismic sequences identified in this study and the ages of their boundaries. The sequence boundaries or unconformity surfaces were correlated at the IIH-1Xa well with those of KIGAM (1997) and Ryu et al. (2000). Ages of the unconformity surfaces were estimated, assuming that the sediment accumulation rates between the key unconformity surfaces were constant.

time-depth conversion. The depth-converted sections or depth models were imported to 2DMove[®] (version 2008.1) for balanced cross-section restoration.

Restoration of the depth models (Fig. 7) was carried out by successfully stripping off (backstripping) each sequence and restoring faults and folds so that the paleo-topography or depositional surface was restored to a continuous layer with topography. The paleo-depositional surface was assumed to be flat because the basin fill in the Kunsan Basin consists dominantly of non-marine sediments. The integrity of the depth models (e.g., horizon termination, attachment of horizons to faults and boundaries, complete closure of polygons, etc) was checked and minor inconsistencies were edited before and after restoring faults and folds. Decompaction correction to account for the loading effect of the removed top sequence was accomplished during backstripping. The porosity-depth relationship for 50% shale/50% sand (Sclater and Christie, 1980) was assumed because the study area is dominated by sand and shale (KIGAM, 1997). If the top horizon is truncated, the truncated layers were restored by projecting the horizons that terminate at the top surface, assuming constant thickness and parallel geometry. Then, faults were restored using the Inclined-Shear module. Shear angles of 60° – 70° gave good results. Unfolding to the paleo-depositional surface was accomplished using the

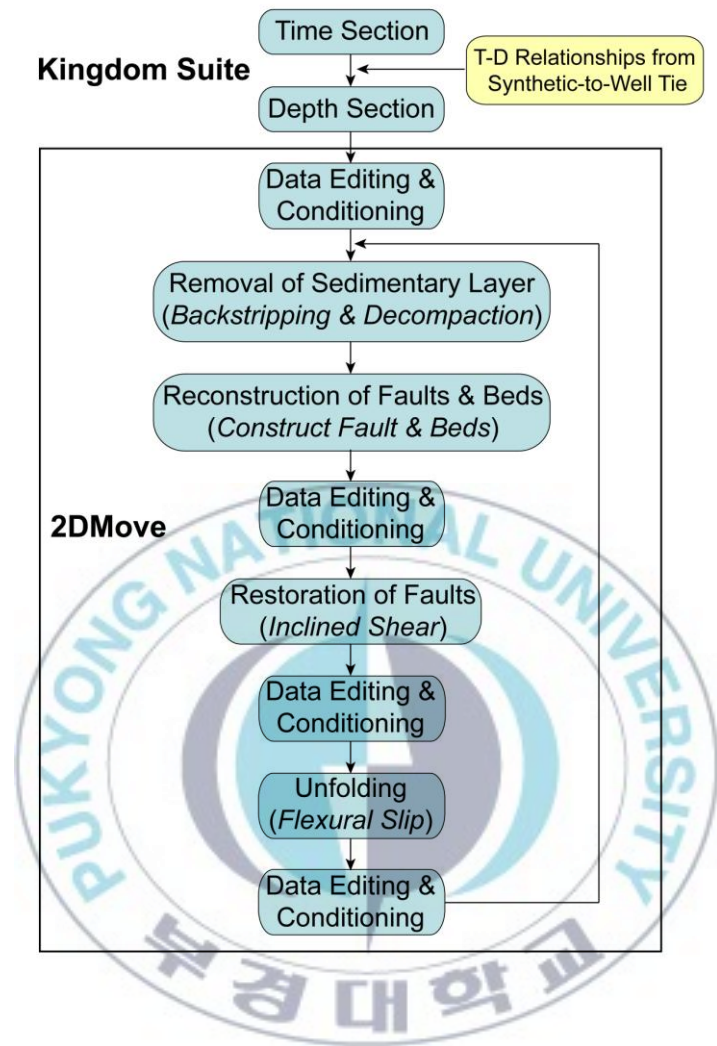


Fig. 7. Cross-section restoration procedure. The depth models for Lines 1 and 2 were constructed from seismic profiles using Kingdom Suite[®]. 2DMove[®] was used for cross-section restoration.

Flexural-Slip module. After unfolding, the new top sequence was backstripped and the same procedure was repeated.



3.2 Results and interpretation

3.2.1 Line 1

Line 1 is about 50 km long and crosses the depocenter of the Central Subbasin and the IHH-1Xa and dummy wells in a NE-SW direction (Figs. 2, 3, 4). A basin began to form in the Late Cretaceous (Fig. 8A) and remained a depocenter throughout the evolution of the Central Subbasin. The large SW-dipping fault bounding the depocenter appears to have rotated, as evidenced by the thickening of sedimentary layers toward the fault (Figs. 8D, E, F), and soled out into the N-dipping regional fault that forms the southern boundary of the Central Subbasin. Extension continued until the Late Oligocene-Early Miocene (Figs. 8F, G) when a local inversion created an anticline-like structure at the IHH-1Xa well location in the northeast. The amount of uplift due to this inversion is estimated to be about 1 km. This local inversion may be related to transpression because crustal shortening was apparently not accompanied. The basin experienced two more inversions in the Early (22-17 Ma)-Middle Miocene (17-13 Ma) (Figs. 8H, I). The 17-13 Ma inversion appears to be very minor. These inversions were also probably due to transpression because crustal shortening is hardly recognizable. These inversions marked the end of the rift phase of the Central Subbasin. Faults were active throughout the rift phase (~ 13 Ma).

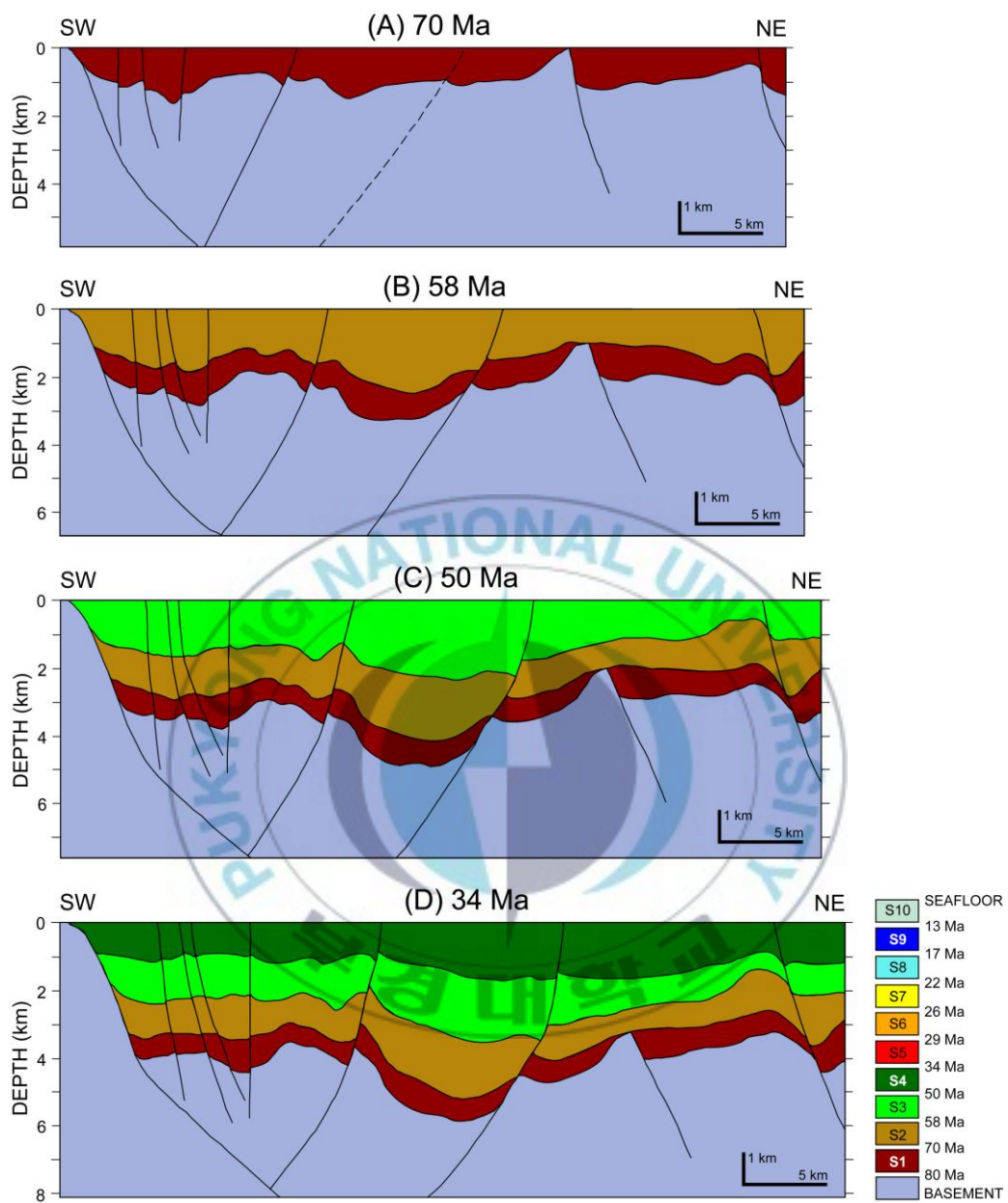


Fig. 8. Sequential restoration of the depth model of Line 1. Vertical exaggeration is approximately 2 \times .

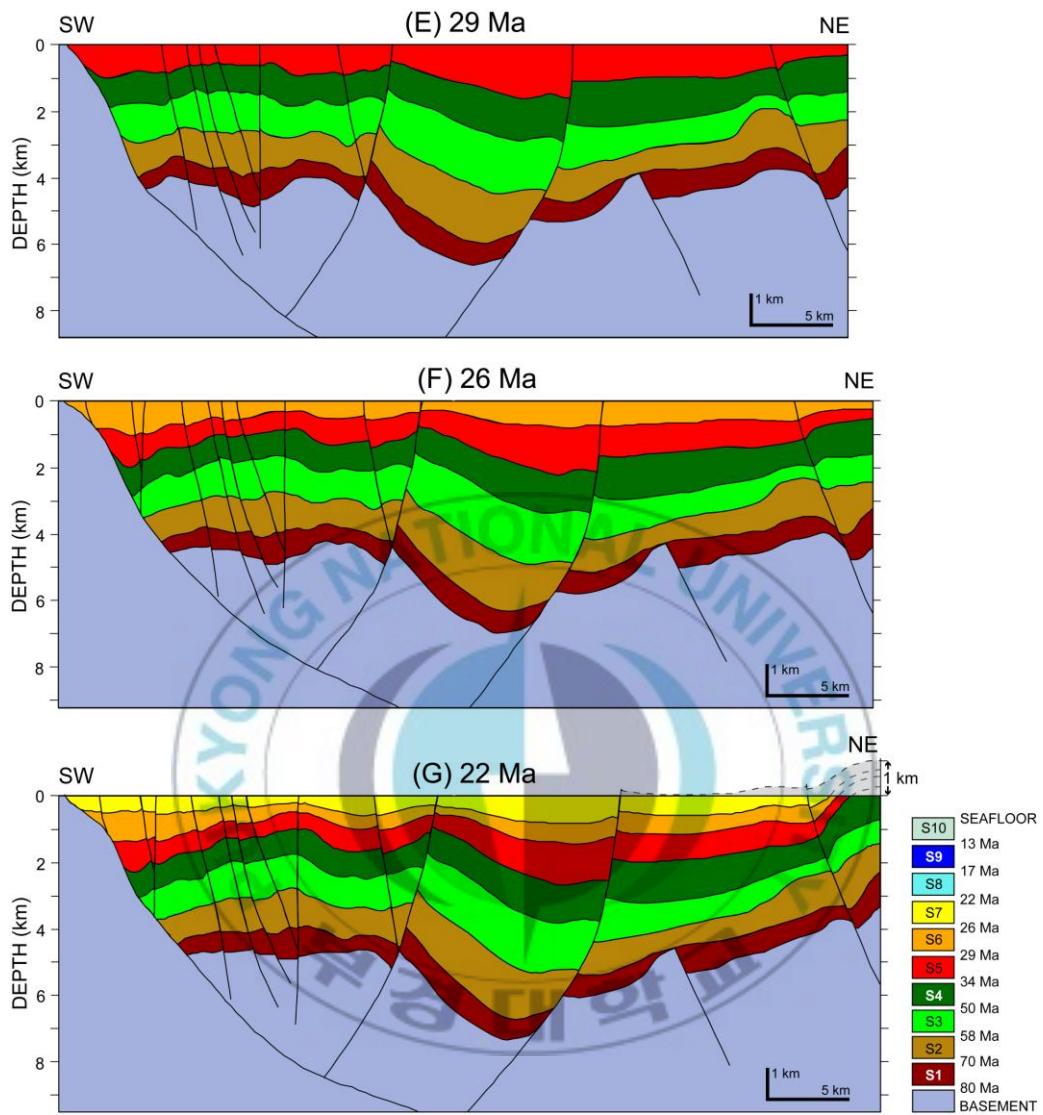


Fig. 8. Continued.

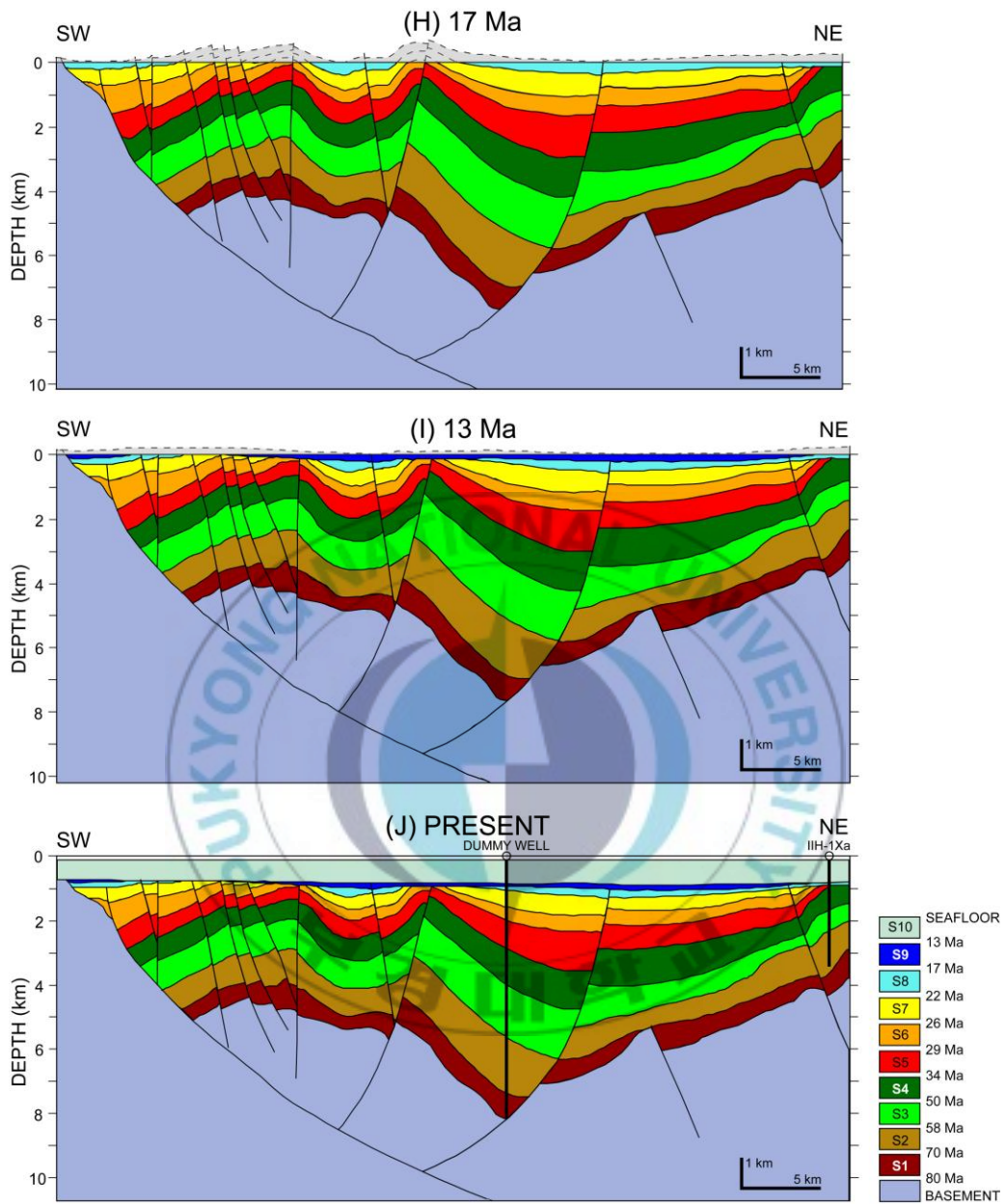


Fig. 8. Continued.

3.2.2 Line 2

Line 2 is about 60 km long and crosses the depocenter of the Central Subbasin and the dummy well in a NW-SE direction (Figs. 2, 3, 5). The large SW-dipping fault bounding the depocenter and the S-dipping faults (see Fig. 3 for fault orientation) in the central part of the depocenter appear to have rotated, soling out into the N-dipping boundary fault along the southern margin of the subbasin. Rotation of the SW- and S-dipping faults resulted in thick sediment accumulation in the downthrown side of the fault (Figs. 9C, D, E). Extension (> 4 km) was greatest during the Paleocene-Early Oligocene (Figs. 9A, B, C). At least two inversions are observed in the Early to Middle Miocene: (1) between 22 Ma and 17 Ma (Figs. 9G, H) and (2) between 17 Ma and 13 Ma (Figs. 9H, I). The 26-22 Ma inversion seen at the IHH-1Xa well location in Line 1 is not observed in Line 2, suggesting that it was local. The magnitude of uplift during the first inversion is estimated to be about 2 km. The second inversion was very mild. The inversions are probably due to transpression or mild compression because crustal shortening is not evident. Faulting continued until the Middle Miocene (Fig. 9I).

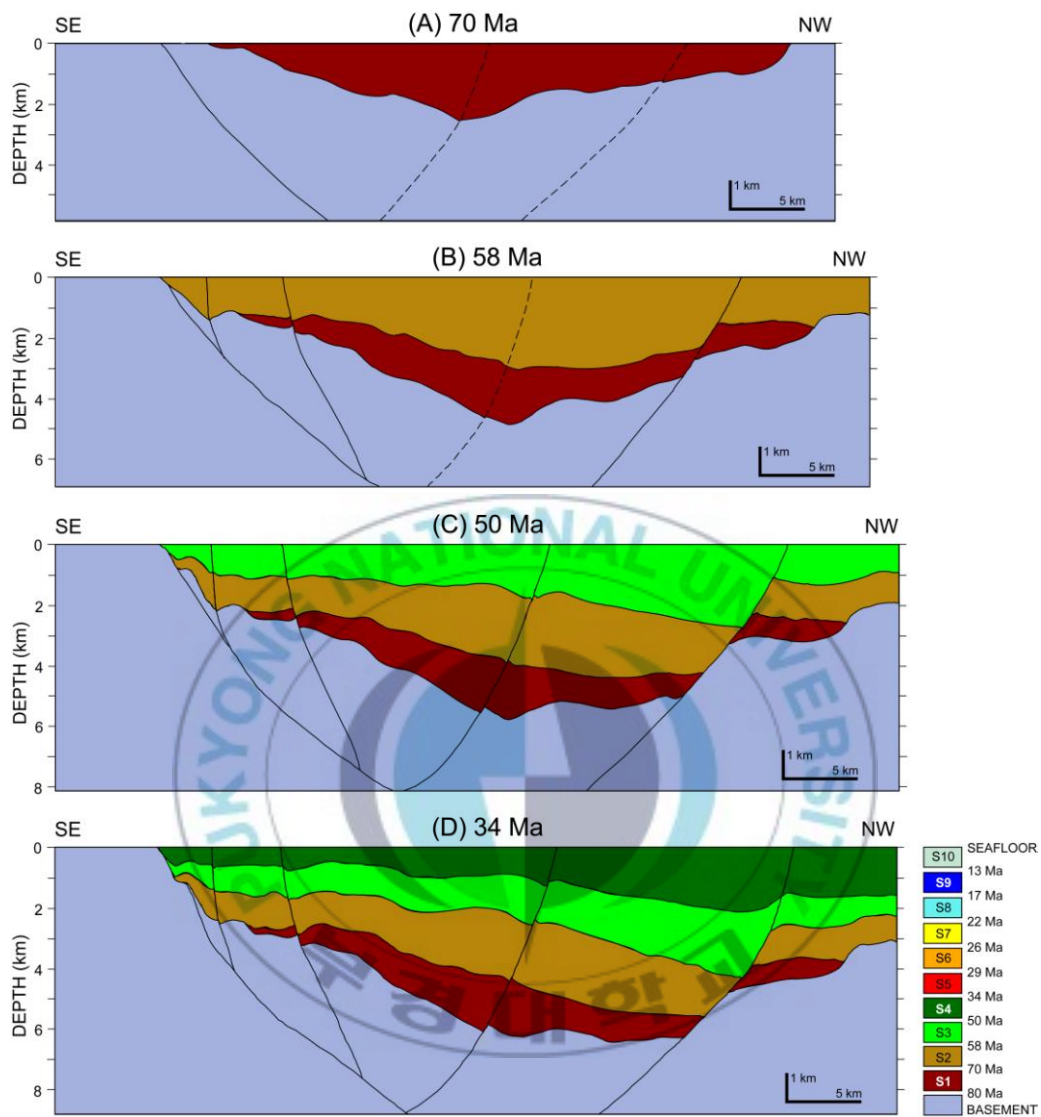


Fig. 9. Sequential restoration of the depth model of Line 2. Vertical exaggeration is approximately 2 \times .

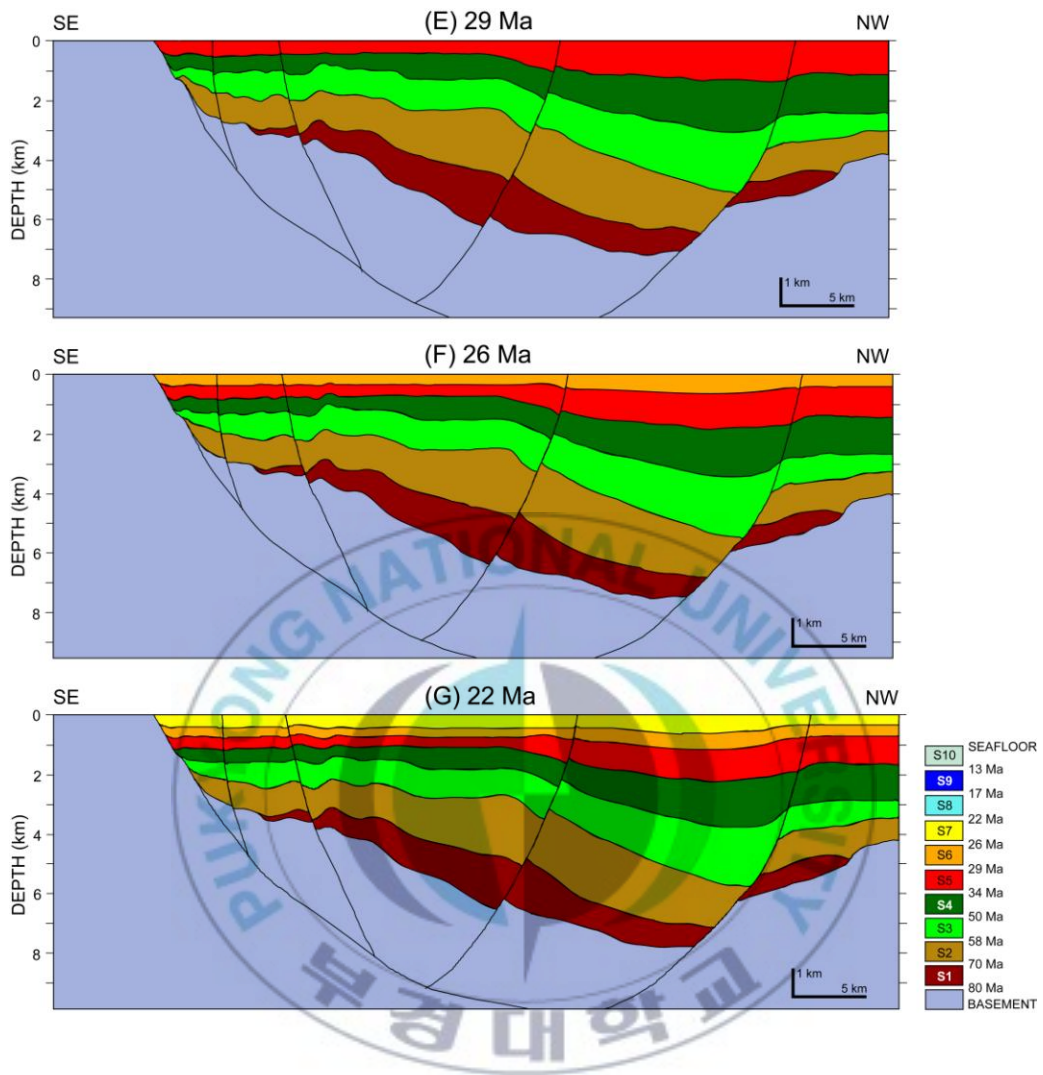


Fig. 9. Continued.

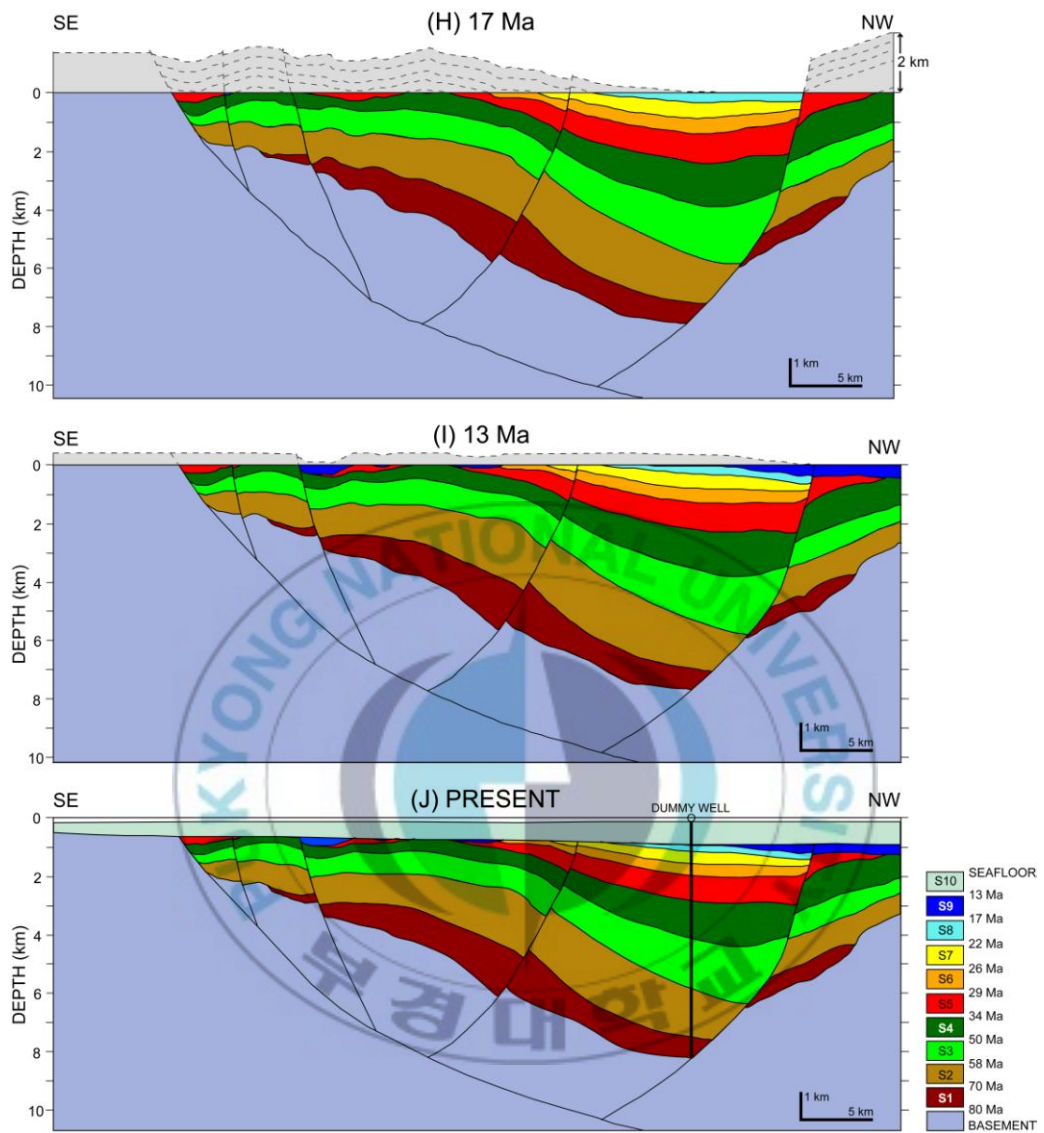


Fig. 9. Continued.

4. Basin modeling

4.1 Methods

Source rocks in continental rift basins include early synrift lacustrine, late synrift nonmarine and fluvio-deltaic, and early postrift marine sediments, as known in many Tertiary rift basins in SE Asia (Doubst and Sumner, 2007). Thus, lacustrine and nonmarine or fluvio-deltaic sediments deposited during the rift phase are potentially the most important source rocks in the Kunsan Basin. In the Subei Basin, the known source rocks are nonmarine sediments, consisting mainly of type III kerogen (TOC 1.08% average) (Wu et al., 2008). In the West Korea Bay Basin, the Eocene sequence contains organic-rich (TOC up to 7%) lacustrine mudstones with a mixture of type I and type III kerogens; the Lower Cretaceous argillaceous sediments are organic-lean (TOC 0.9% average) and contain gas-prone type III kerogen (Massoud et al., 1991).

The depocenter of the Central Subbasin in Lines 1 and 2 was analyzed for seismic facies to interpret lacustrine and nonmarine/fluvial sediments (Figs. 5, 10). Lacustrine sediments are commonly characterized by high-amplitude, locally continuous reflections (Dempsey, 1996; Girardclos et al., 2008), whereas nonmarine/fluvial sediments are characterized by variable amplitude reflections with poor continuity (Mitchum et al., 1977). The seismic facies, interpreted as lacustrine sediments with type I kerogen in Lines 1 and 2, are

characterized by moderate- to high-amplitude, locally continuous reflections, onlapping onto the underlying layer (Fig. 10A). Because typical nonmarine/fluvial seismic facies (e.g., variable amplitude reflections with low continuity) (Fig. 10B) occur at many stratigraphic levels, the nonmarine/fluvial seismic facies with two-way travel time thickness greater than 25 ms were assumed to have source rock potential with type III kerogen. The depocenter of the Central Subbasin contains source rocks at six stratigraphic levels that include four lacustrine (source rocks #1, 3, 5, and 6) and two nonmarine/fluvial layers (source rocks #2 and 4) (Fig. 11A). Seismic facies in the southern part of the Central Subbasin away from the dummy well were not interpreted because of the poor data quality.

The IHH-1Xa well was also used in basin modeling to include the depocenter margin. Good source rocks were not encountered at the IHH-1Xa well (KIGAM, 1997). The Middle Eocene and younger rocks contain type III kerogen of low (< 0.5%) TOC. The older rocks are nearly kerogen-free. To model the entire sedimentary section at the depocenter margin, the IHH-1Xa well was extended beyond the actual bottom depth (3,467 m) to the acoustic basement (4,365 m) (Fig. 11B). We assumed that lacustrine sediments with type I kerogen are present in S1 at the IHH-1Xa well as the well penetrated the

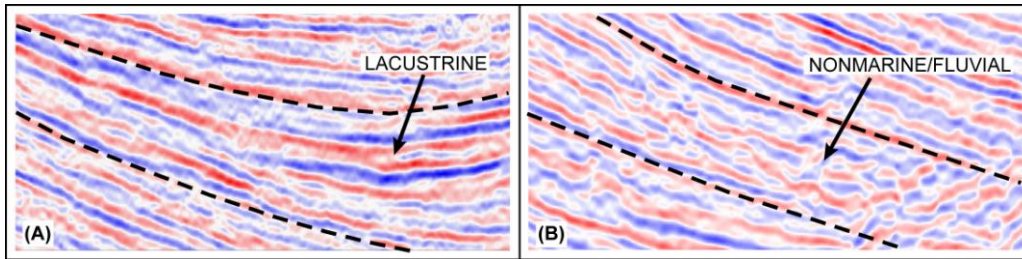
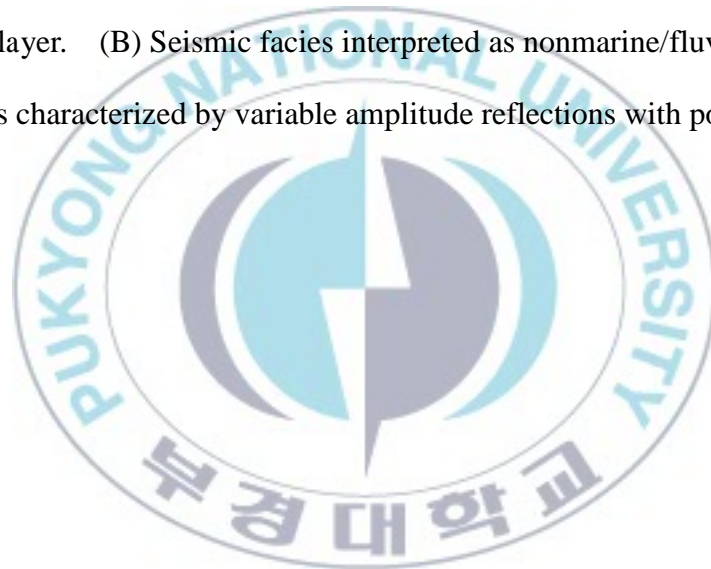


Fig. 10. (A) Seismic facies interpreted as lacustrine sediments is characterized by moderate- to high-amplitude, continuous reflections, onlapping onto the underlying layer. (B) Seismic facies interpreted as nonmarine/fluviol sediments is characterized by variable amplitude reflections with poor continuity.



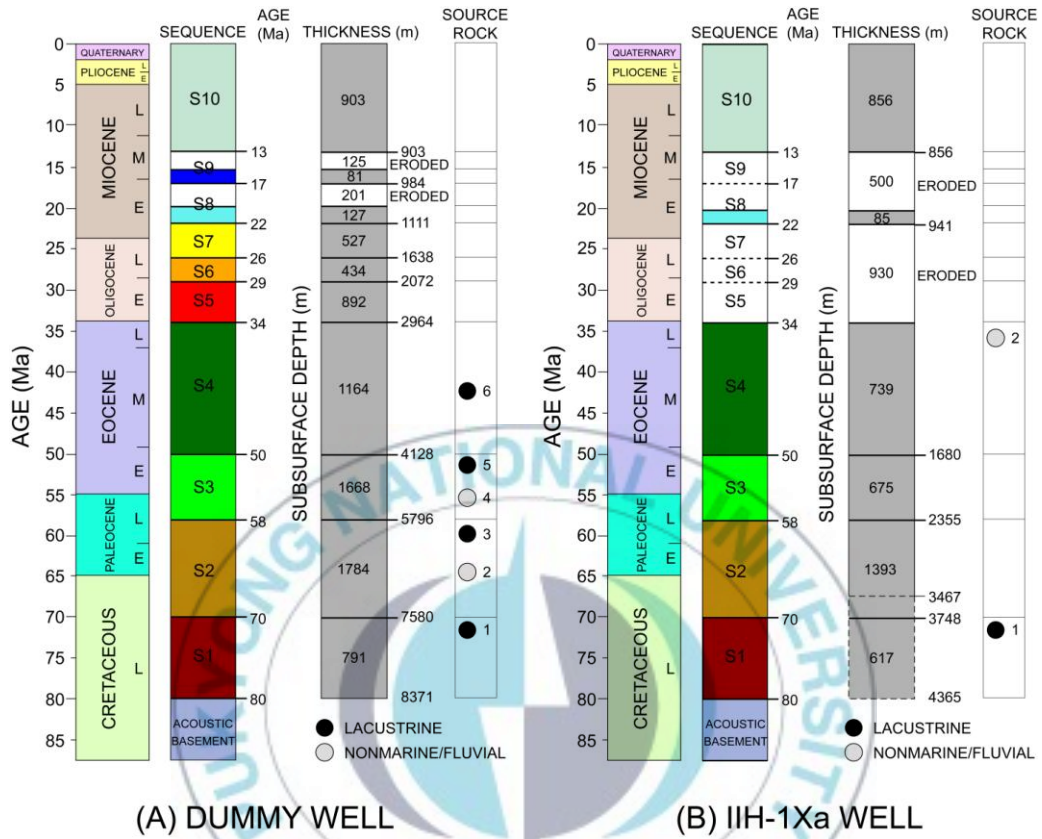


Fig. 11. (A) Stratigraphic column, thicknesses of ten sequences, and source rock locations of the dummy well. (B) Stratigraphic column, thicknesses of ten sequences, and source rock locations of the IIH-1Xa well. The IIH-1Xa well was extended beyond the actual bottom depth (3,467 m) to the basement (4,365 m) to include the deep source rocks in basin modeling.

thickest part of the downthrown side of the N-dipping fault where lakes were probably formed (Figs. 8B, C). Type III kerogen was also assumed in the Middle-Late Eocene section at IHH-1Xa well. The depths of the unconformities and the top of the acoustic basement (Fig. 11) at the dummy and IHH-1Xa wells, which are the important input parameters for basins modeling, were obtained from the cross-section restoration.

The stratigraphy versus time (subsidence history) and thermal history for the dummy and IHH-1Xa wells were modeled using GENEX[®] (version 4.0.3), which is a numerical simulation program for one-dimensional basin modeling. Procedures in GENEX[®] basin modeling include: (1) backstripping and decompaction, (2) temperature reconstruction, and (3) kinetic modeling. GENEX[®] can compute the detailed thermal maturity of source rocks and the amount of expelled and residual hydrocarbons. However, we examined only the subsidence and petroleum generation/expulsion histories because the quantitative data for source rocks are unavailable. The three fraction kinetic model (Beicip-Franlab, 1995) was used to reproduce the influence of time and temperature on hydrocarbon generation and expulsion.

Most input parameters involved in basin modeling generally have varying degrees of uncertainty (Poelchau et al., 1999). The key input parameters for the basin modeling for the dummy and IHH-1Xa wells are listed in Table 1.

Table 1. The key input parameters for one-dimensional basin modeling.

Parameter	Dummy well	IIH-1Xa well	Reference
Initial basement thickness [km]	35	35	Waples, 2001
Temperature before 5 Ma [°C]	15	15	Korea Meteorological Administration, 2009
Temperature after 5 Ma [°C]	8	8	Kang and Kim, 2008
Present-day heat flow [mW/m ²]	65	65	Han and Keehm, 1996
Source rock kerogen type (TOC)	Type III (1%) Type I (2%)	Type III (1%)	Wu et al., 2008 Katz and Xingcai, 1998



Default values were used for some of the other input parameters that are either usually unknown (e.g., basal heat flow, pressure regime) or adjusted within reasonable boundaries to fit observations (e.g., crustal density and conductivity) (Beicip-Franlab, 1995). The initial crustal thickness was assumed to be 35 km, a typical value for the continental crust (Waples, 2001). The surface temperature before 5 Ma was assumed to be 15°C (Korea Meteorological Administration, 2009) which is the annual average temperature in Kunsan, a port city in western Korea close to the study area because the Kunsan Basin was in a nonmarine environment until the Pliocene (ca. 5 Ma) (Li, 1984). The surface temperature since the Pliocene was assumed to be the present-day bottom-water temperature (8 °C) (Kang and Kim, 2008). The heat flow (65 mW/m²) was taken from the present-day heat flow distribution in the Central Subbasin, predicted from the spherical harmonic method (Han and Keehm, 1996). The TOC of the type I and type III kerogens are assumed to be 2% and 1%, respectively (Katz and Xingcai, 1998; Wu et al., 2008).

4.2 Results and interpretation

Oil generation at the dummy well location began as early as in the Late Paleocene from the deep source rocks and in the Late Oligocene from the shallow source rocks (Fig. 12A). Expulsion of hydrocarbons, mostly oil, at the dummy well location began in the Early Eocene from the deep source rocks and in the Late Oligocene-Early Miocene from the shallow source rocks (Fig. 12B). However, most source rocks at the dummy well location passed the main expulsion phase except for the shallowest source rock (source #6) (Fig. 12C). The volumes of hydrocarbons expelled from the nonmarine/fluvial source rocks (source rocks # 2, 4) were very small.

Oil generation at the IIH-1Xa well location began in the Early Eocene from the deep source rock with type I kerogen and continues today (Fig. 13A). The shallow source rocks are thermally immature. Hydrocarbon expulsion from the deep source rocks at the IIH-1Xa well location began in the Middle Eocene and peaked in the Early Oligocene (Fig. 13B). Only very small amounts of hydrocarbons are currently being expelled from the deep source rocks at the IIH-1Xa well location (Fig. 13C).

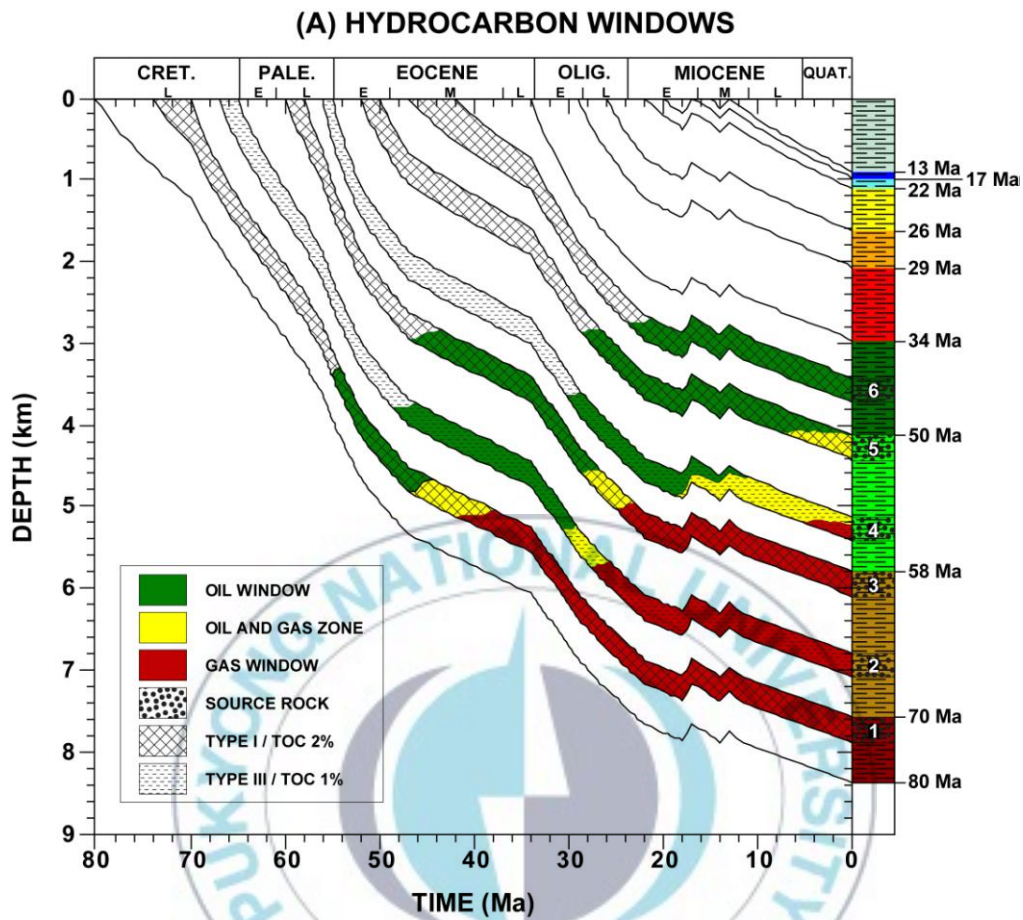


Fig. 12. (A) Burial history and hydrocarbon windows; (B) burial history and expulsion windows; and (C) expelled hydrocarbons per time interval for the dummy well. Oil generation began in the Late Paleocene from the deep source rocks and in the Late Oligocene from the shallow source rocks. Most source rocks passed the main expulsion phase except for the shallowest source rock (source #6). The volumes of hydrocarbons expelled from the nonmarine/fluvial source rocks (source rocks # 2, 4) were very small.

(B) EXPULSION WINDOWS

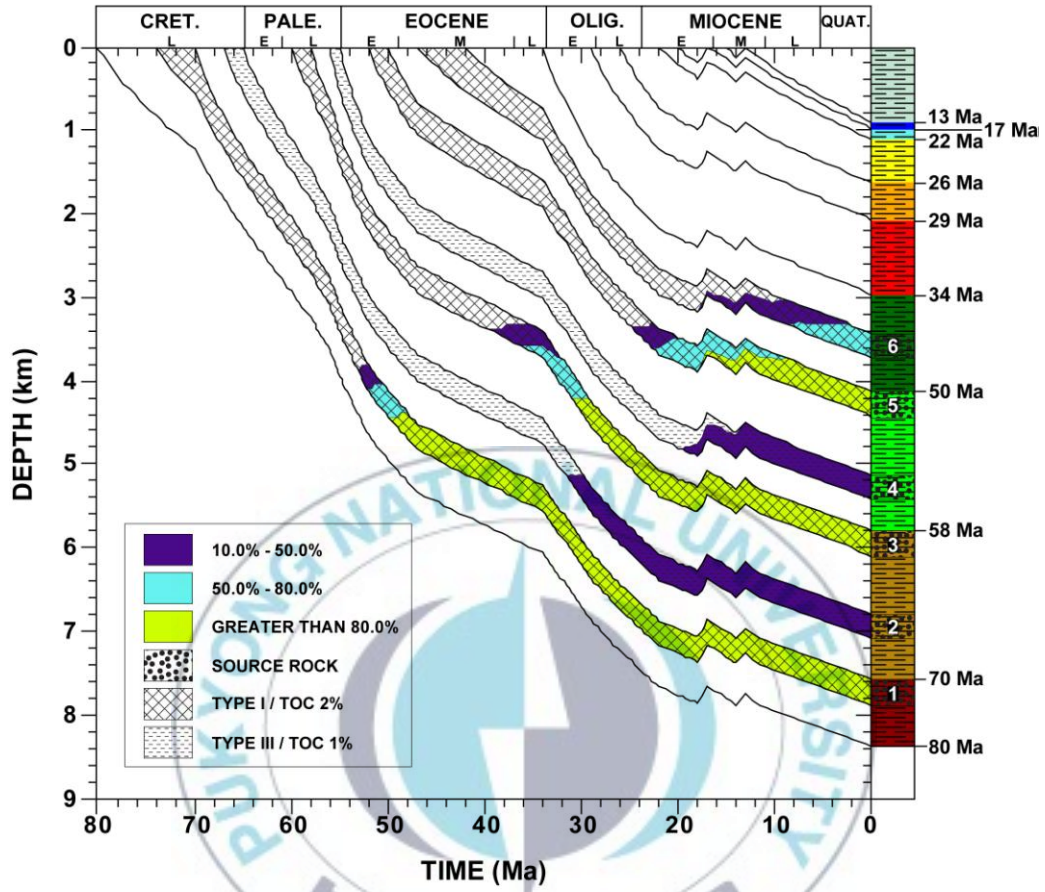


Fig. 12. Continued.

(C) EXPELLED HC PER TIME INTERVAL

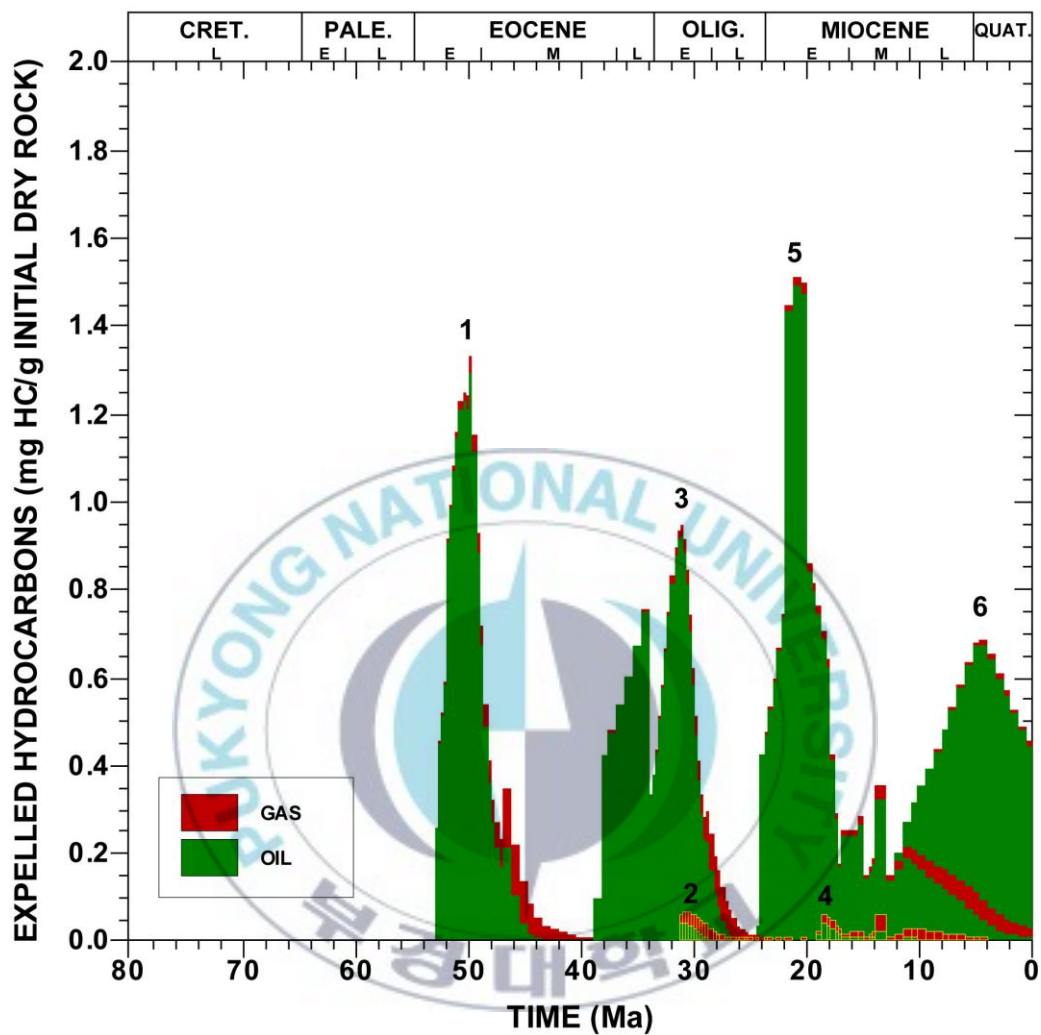


Fig. 12. Continued.

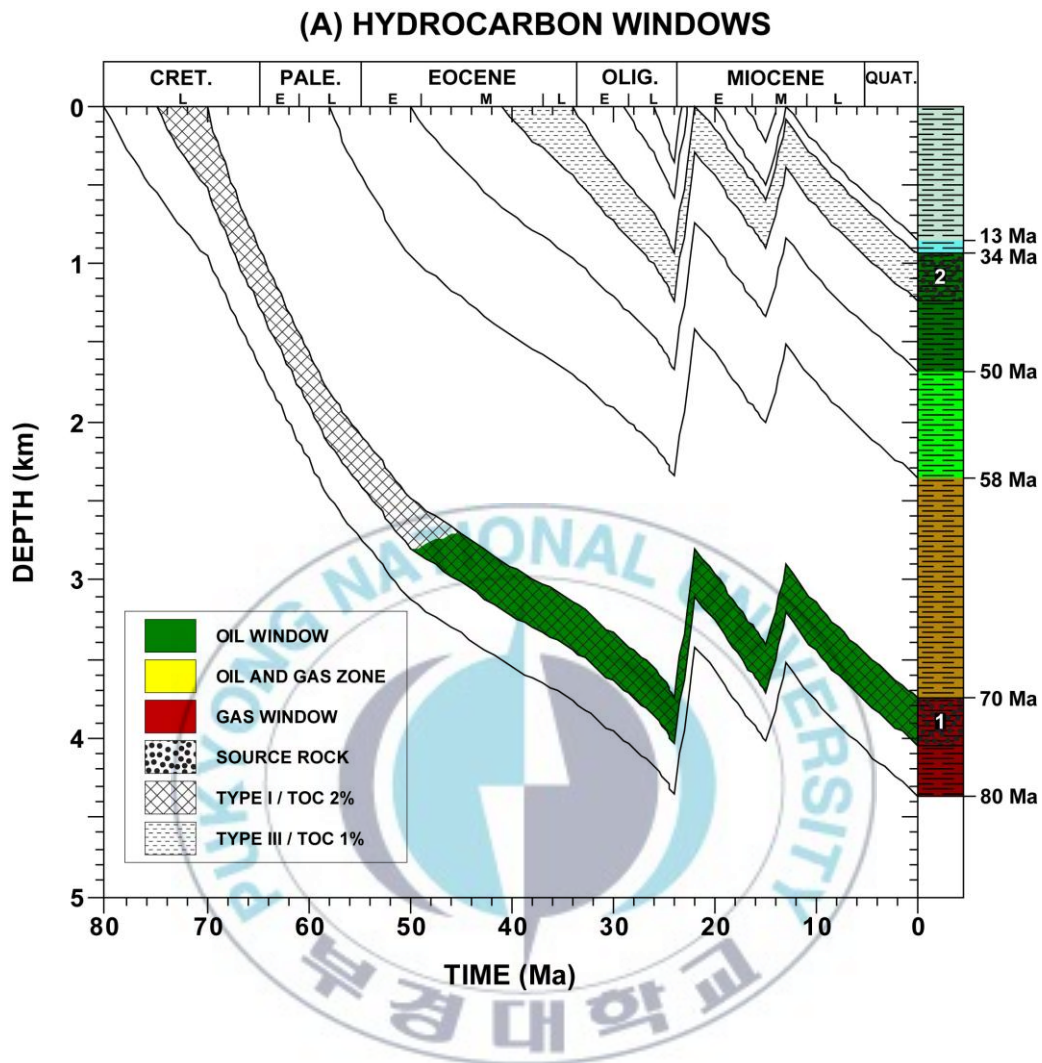


Fig. 13. (A) Burial history and hydrocarbon windows; (B) burial history and expulsion windows; and (C) expelled hydrocarbons per time interval for the IIIH-1Xa well. Hydrocarbon expulsion from the deep source rocks began in the Middle Eocene and peaked in the Early Oligocene. Only very small amounts of hydrocarbons are currently being expelled from the deep source rocks.

(B) EXPULSION WINDOWS

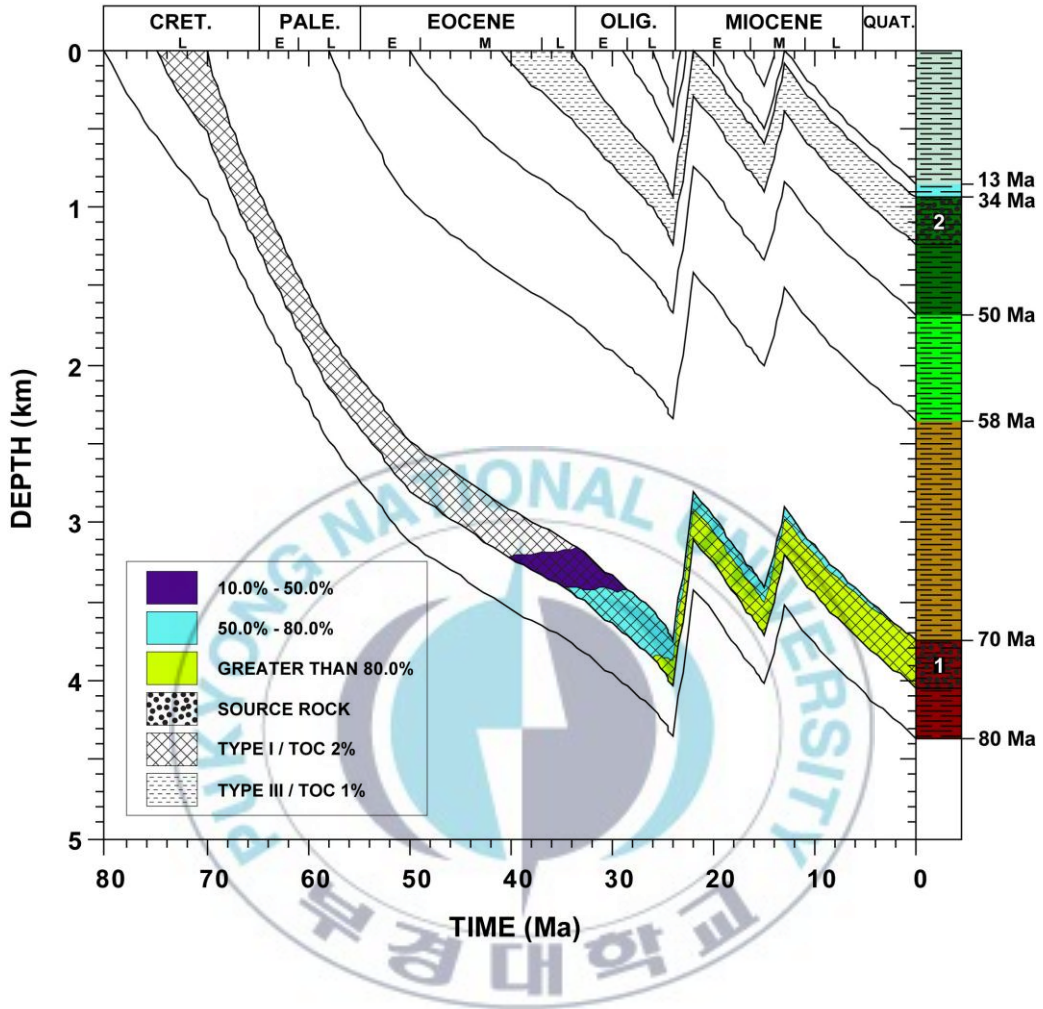


Fig. 13. Continued.

(C) EXPELLED HC PER TIME INTERVAL

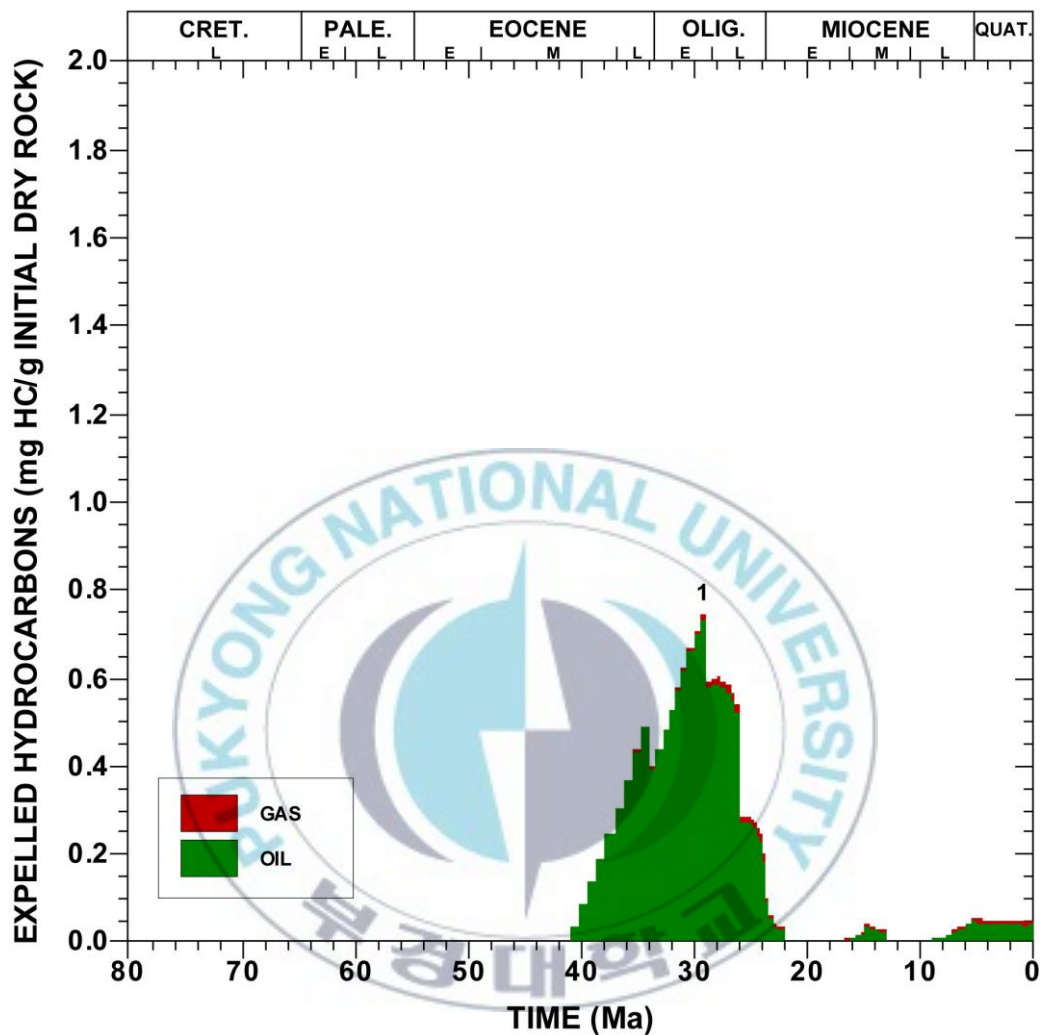


Fig. 13. Continued.

5. Discussion

Rift basins include over 170 of the world's largest hydrocarbon accumulations greater than 500×10^6 barrels of oil or over 3×10^{12} ft³ of gas (Mann et al., 2001), comprising about one third of discovered global hydrocarbon resources (Fraser et al., 2007). Many hydrocarbon-rich Tertiary basins in Southeast Asia are continental rift basins (Hall, 2009). The Yellow Sea also consists of Tertiary continental rift basins with thick basin fill. The cross-section restoration and basin modeling for the Central Subbasin in the Kunsan Basin have provided, for the first time, constraints on the timings of trap formation and hydrocarbon generation/expulsion in the area (Fig. 14).

The cross-section restoration suggests inversions in the Late Oligocene-Middle Miocene that created anticlinal structures. The inversions largely postdated the main phase of hydrocarbon expulsion and charge in the northeastern margin of the depocenter of the Central Subbasin but predated the hydrocarbon expulsion and charge from the shallow source rocks in the depocenter of the subbasin. The hydrocarbons generated from the depocenter of the subbasin were likely to have migrated preferentially toward the anticlinal structure and faults in the south away from the northern and northeastern margins of the depocenter of the subbasin because the basin-fill strata are

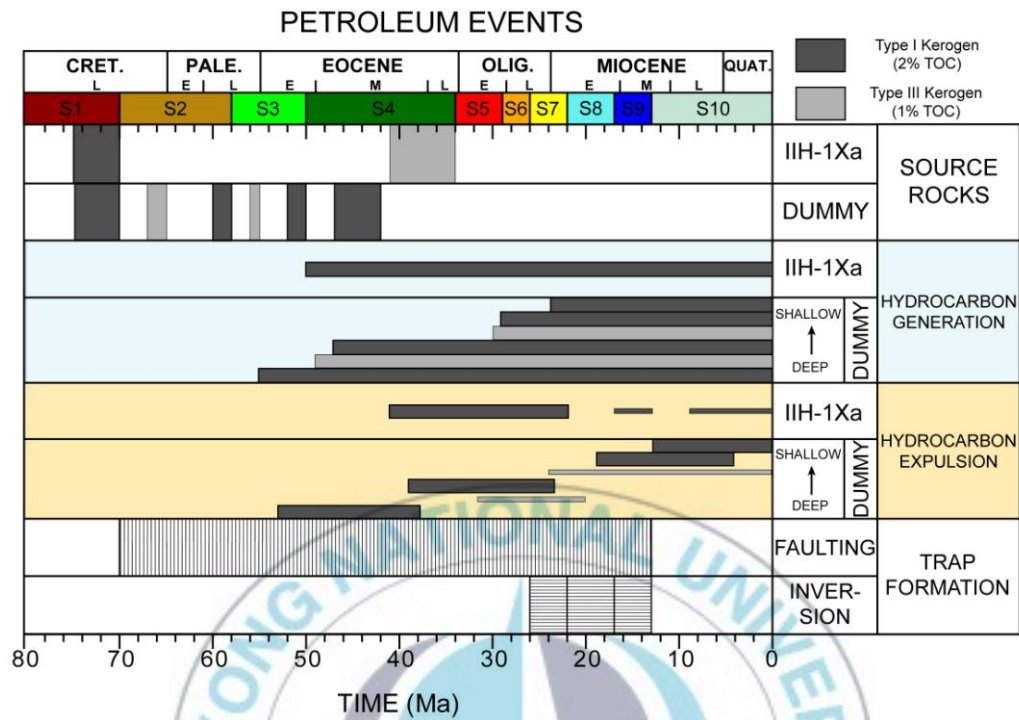
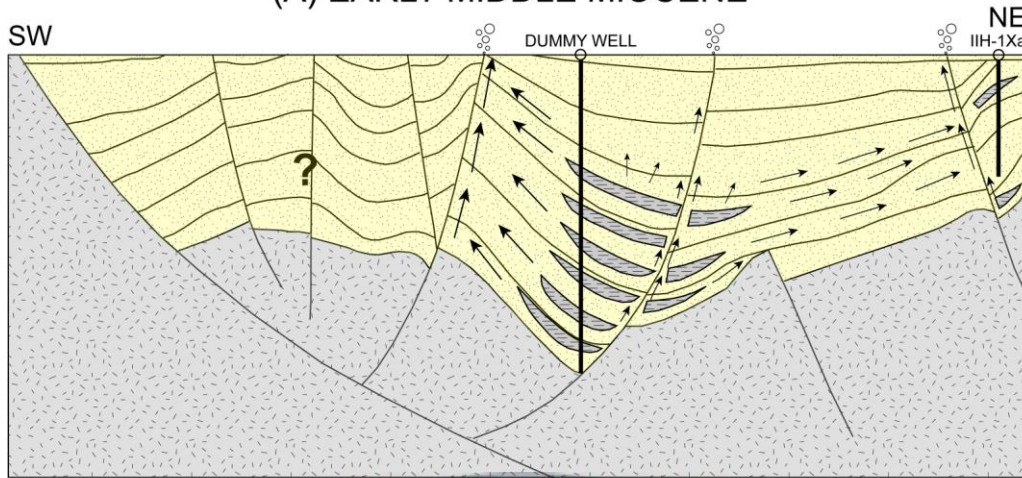


Fig. 14. Petroleum event chart for the Central Subbasin. The inversions largely postdated the main phase of hydrocarbon expulsion in the northeastern margin of the depocenter of the subbasin but predated the hydrocarbon expulsion from the shallow source rocks in the depocenter of the subbasin. Faults remained active until the Middle Miocene.

dipping north (Fig. 15). However, most of these hydrocarbons probably leaked through the faults during the rift phase of the subbasin (~ Middle Miocene) when faulting remained active (Fig. 15A). Some hydrocarbons from the deep parts of the subbasin to the north of the large SW-dipping fault probably migrated northward but these hydrocarbons were probably intercepted by the N-dipping fault immediately south of the anticline, penetrated by the IIIH-1Xa well (Fig. 15A).

The cessation of faulting sometime in the Middle Miocene probably had significant impact on the trapping potential in the area as inactive or dead faults can act as a seal (Fig. 15B). Hydrocarbons from the shallower source rocks in the depocenter of the subbasin have migrate southward and may be curently filling the anticlinal structure and associated fault traps (Fig. 15B). This anticlinal structure and associated fault traps have never been tested. Hydrocarbons from the thick sediment fill to the north of the large SW-dipping fault probably have migrated northward. These hydrocarbons are not likely to have spilled across the N-dipping fault immediately south of the IIIH-1Xa well, and may be trapped against the fault. Because faults in the area not only created traps but probably also acted as conduits for the escape of hydrocarbons, a detailed fault study is necessary to better understand the role of the faults in the area.

(A) EARLY-MIDDLE MIOCENE



(B) PRESENT

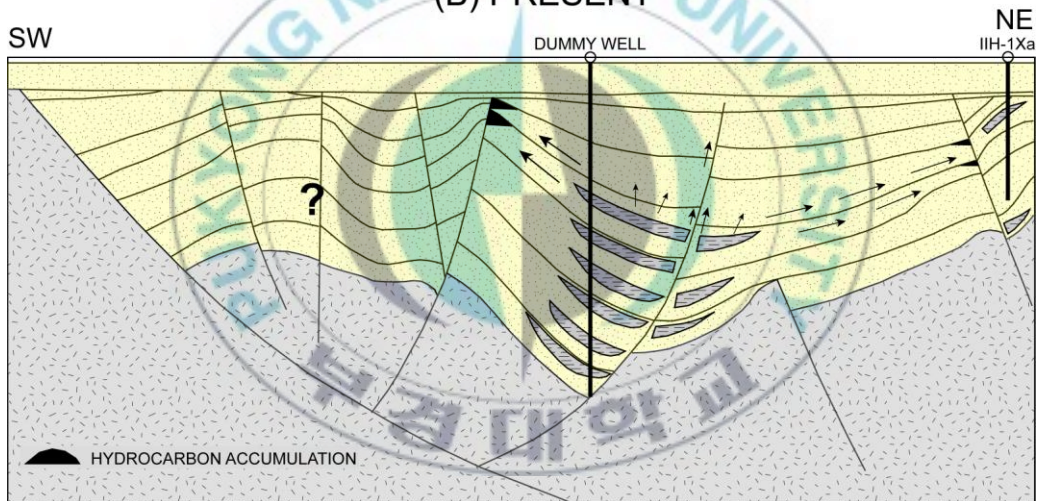


Fig. 15. (A) Schematic cross-sectional diagram showing hydrocarbon migration for Oligocene-Middle Miocene time. Hydrocarbons from the depocenter of the Central Subbasin migrated preferentially toward the anticlinal structure and faults in the south. However, most of these hydrocarbons leaked through the faults during the rift phase of the subbasin (~ Middle Miocene) when faulting remained active. Hydrocarbons from the deep parts of the subbasin to the north of the large SW-dipping fault migrated northward but were probably intercepted by the fault immediately south of the anticline penetrated by the IHH-1Xa well. (B) Schematic cross-sectional diagram showing hydrocarbon migration for the present day. Cessation of faulting sometime in the Middle Miocene had significant impact on the trapping potential. Hydrocarbons from the shallow source rocks in the deepest part of the subbasin have migrated southward and may be filling the anticlinal structure and associated fault traps to the south of the dummy well. Hydrocarbons from the thick sediment fill to the north of the large SW-dipping fault probably have migrated northward and may be accumulating against the fault south of the IHH-1Xa well.

6. Summary and conclusions

- Cross-section restoration and basin modeling have provided, for the first time, constraints on the timings of trap formation and hydrocarbon generation/expulsion in the Kunsan Basin.
- Extension with downfaulting and rotation of the basin fill continued in the Central Subbasin until the Late Oligocene-Early Miocene.
- Extension was terminated by inversions in the Early to Middle Miocene, which were probably due to transpression or mild compression.
- Hydrocarbon expulsion in the depocenter began in the Early Eocene and continues today; however, most source rocks passed the main expulsion phase except for the shallowest source rock.
- Hydrocarbon expulsion in the northeastern margin of the depocenter of the subbasin began in the Middle Eocene and peaked in the Early Oligocene; only very small amounts of hydrocarbons are currently being expelled from the deep source rocks.
- The inversions that created traps largely postdated the main phase of hydrocarbon expulsion in the northeastern margin of the depocenter of the subbasin but predated the hydrocarbon expulsion from the shallow source rocks in the depocenter of the subbasin.
- Hydrocarbons generated from the depocenter of the subbasin are likely to

have migrated southward toward the anticlinal structure, away from the traps in the north because of the N-dipping basin-fill strata. The anticlinal structure and faults to the south of the dummy well have never been tested.



Acknowledgements

I would like to express my sincere thanks to my supervisor Prof. Gwang Hoon Lee who gave me numerous helpful suggestions, important advice and constant encouragement from undergraduate years. I am also grateful to Prof. Dae Choul Kim, Prof. Jeong Gi Um, Prof. Ki Ha Lee and Prof. Seon-Ok Kim for their guidance.

I greatly appreciate my current and former colleagues in the energy exploration lab, Sang Hoon Han, Boyeon Yi, Heon Hak Lim, Seong Min Nam, Hyewon Sa, Senay Horozal, Ibrahim Ilhan, and Ayse Gungor. I am also thankful to Byong Hoon Nam who is in heaven for his advice and encouragement. I also thank Sang Bae Lee, Ki Han Woo, Han Ki Kim, In Sill Heo, Ja Hoon Koo, Byung Joon Hwang, Do Ha Kim, Gwang Soo Lee, Jae Wook Suk, Jung Min Jang and Hannuree Jang for their friendship.

Finally, I am extremely thankful for my parents and my brother for their love, continuous encouragement and support.

References

- Beicip-Franlab (1995). User's guide: GENEX for Windows. Rueil-Malmaison: Beicip Franlab (not paginated).
- Barry, T.L., Kent, R.W., 1998. Cenozoic magmatism in Mongolia and the origin of central and East Asia basalts. In: Flower, M., Chung, S.L., Lo, C.H. (Eds.), *Mantle Dynamics and Plate Interactions in East Asia*. American Geophysical Union Geodynamics Series 27, pp. 347-364.
- Dempsey, C., 1996, Interpreter's corner: The Leading Edge 15, 716-718.
- Doust, H., Sumner, H.S., 2007. Petroleum systems in rift basins – a collective approach in Southeast Asian basins. *Petroleum Geoscience* 13, 127-144.
- Fraser S.I., Fraser, A.J., Lentini, M.R., Gawthorpe, R.L., 2007. Return to rifts – the next wave: fresh insights into the petroleum geology of global rift basins. *Petroleum Geoscience* 13, 99-104.
- Gilder, S., Courtillot, V., 1997. Timing of the North-South China collision from the middle to late Mesozoic aleomagnetic data from the North China Block. *Journal of Geophysical Research* 102, 17713-17727.
- Girardclos, S., Fiore, J., Rachoud-Schneider, A.-M., Baster, I., Wildi, W., 2008. Petit-Lac (western Late Geneva) environment and climate history from deglaciation to the present: a synthesis. *BOREAS* 34, 417-433.
- Hall, R., 2009. Hydrocarbon basins in SE Asia: understanding why they are

- there. *Petroleum Geoscience* 15, 130-146.
- Han, S.H., 2008. Structural evolution of the Kunsan basin, southern Yellow Sea. MS thesis, Pukyong National University, Busan. 59 pp.
- Han, U., Keehm, Y S., 1996. A Study on the Heat Flow Distribution in the Korean Peninsula and its vicinity. *Journal of Geological Society of Korea* 32, 267-275.
- Hao, F., Zhou, X., Zhu, Y., Zou, H., Bao, X., and Kong, Q., 2009. Mechanisms of petroleum accumulation in the Bozhong sub-basin, Bohai Bay Basin, China. Part 1: Origin and occurrence of crude oils. *Marine and Petroleum Geology* 26, 1523-1542.
- Hsü , K.J., 1989. Origin of sedimentary basins of China. In: Zhu, X. (Ed.), *Chinese Sedimentary Basins. Sedimentary Basins of the World 1*. Elsevier, New York, pp. 208-227.
- Kang, J. H., Kim, W. S., 2008. Spring dominant copepods and their distribution pattern in the Yellow Sea. *Ocean Science Journal* 43, 67-79.
- Katz, B. J., Xingcai, L., 1998. Summary of the AAPG Research Symposium on lacustrine basin exploration in China and Southeast Asia. *American Association of Petroleum Geologists Bulletin* 82, 1300-1307.
- KIGAM, 1997. Petroleum Resources Assessment. Korea Institute of Geoscience and Mineral Resources Report KR-97(C)-17, pp. 71-190 (in Korean with English abstract).

Kim, J.-N., Ree, J.-H., Kwon, S.-T., Park, Y., Choi, S.-J., Cheong, C.-S., 2000.

The Kyonggi shear zone of the central Korean Peninsula: late orogenic imprint of the North and South China collision. *The Journal of Geology* 108, 469-478.

Korea Meteorological Administration, 2009. Weather Data of Korea.

http://www.kma.go.kr/sfc/sfc_03_05.jsp (Korea Meteorological Administration website) (accessed August 2009).

Lee, C.S., McCabe, R., 1986, The Banda-Celebes-Sulu basin: a trapped piece of Cretaceous-Eocene oceanic crust? *Nature* 322, 51-54.

Lee, G.H., Kwon, Y.I., Yoon, C.S., Kim, H.J., Yoo, H.S., 2006. Igneous complexes in the Southeastern Northern South Yellow Sea Basin and their hydrocarbon Implications. *Marine and petroleum Geology* 23, 631-645.

Li, D., 1984. Geologic evolution of petroliferous basins on continental shelf of China. *American Association of Petroleum Geologists Bulletin* 68, 993-1003.

Li, D., 1995. Hydrocarbon habitat in the Songliao rift basin, China. In: Lambiase, J. (Ed.), *Hydrocarbon Habitat in Rift Basins*. Geological Society Special Publication 80, pp. 317–329.

Liu, H., 1986. Geodynamic scenario and structural styles of Mesozoic and Cenozoic basins in China. *American Association of Petroleum Geologists Bulletin* 70, 377–395.

- Liu, X., Yang, X., Liu, Y., 2007. Exploration strategies for complex fault block reservoirs in the Subei Basin. *Petroleum Science* 4, 61.
- Man, P., Gahagan, L., Gordon, M., 2001. Tectonic setting of the world's giant oil fields. *World Oil*, September, 42-50; October, 78-84; November, 56-60.
- Massoud, M.S., Killops, S.D., Scott, A.C., Matthey, D., 1991. Oil source rock potential of the lacustrine Jurassic Sim Uuju Formation, West Korea Bay Basin. Part I: Oil source rock correlation and environment of deposition. *Journal of Petroleum Geology* 14, 365-385.
- Massoud, M.S., Scott, A.C., Matthey, D., Keeley, M.L., 1993. Oil source rock potential of the lacustrine Jurassic Sim Uuju Formation, West Korea Bay Basin. Part II: Nature of the organic and hydrocarbon-generation history. *Journal Petroleum Geology* 16, 265-284.
- Mitchum, Jr., R.M., Vail, P.R., Sangree, J.B., 1977. Seismic stratigraphy and global changes of sea level, part 6: Stratigraphic interpretation of seismic reflection patterns in depositional sequences. In: Payton, C.E. (Ed.), *Seismic stratigraphy-applications to hydrocarbon exploration*. American Association of Petroleum Geologists Memoir 26, pp. 117-133.
- Poelchau, H. S., Zwach, C., Hantschel, T., Welte, D. H., 1999. Effect of oil and gas saturation on simulation of temperature history and maturation. In: Forster, A., Merriam, D.F. (Eds.), *Geothermics in Basin Analysis*. Kluwer/Plenum Press, Dordrecht/New York, pp. 219-235.

- Ree, J.H., Cho, M., Kwon, S.T., and Nakamura, E., 1996. Possible eastward extension of Chinese collision belt in South Korea: the Imjingang Belt. *Geology* 24, 1071-1074.
- Ryu, I.C., Kim, B.Y., Kwak, W.J., Kim, G.H., Park, S.J., 2000. Stratigraphic response to tectonic evolution of sedimentary basins in the Yellow Sea and adjustment area. *Korean Journal of Petroleum Geology* 8, 19-26 (in Korean with English abstract).
- Sclater, J.G, Christie, P.A.F., 1980. Continental stretching: an explanation of the post-mid-Cretaceous subsidence of the Central North Sea basin. *Journal of Geophysical Research* 85, 3711-3739.
- Shin, K.S., 2005. Hydrocarbon potential of the Yellow Sea Kunsan Basin. *Seabed Petroleum in Northeast Asia: Conflict or Cooperation*. Woodrow Wilson International Center for Scholars, pp. 54-57.
- Tapponnier, P., Peltzer, G., Armijo, R., Le Dain, A.-Y., Cobbold, P., 1982. Propagating extrusion tectonics in Asia: New insights from simple experiments with plasticine. *Geology* 10, 611–616.
- Waples, D.W., 2001. A new model for heat flow in extensional basins: Radiogenic heat, asthenospheric heat, and the McKenzie model. *Natural Resources Research* 10, 227-238.
- Wu, S., 2002. Mesozoic-Cenozoic rifting and origins of the North Yellow Sea Basin. *Continent–Ocean Interactions within the East Asian Marginal Seas*.

American Geophysical Union Chapman Meeting Abstracts, San Diego, 10–14 November 2002, p. 42.

Wu, S., Ni, X., Cai, F., 2008. Petroleum geological framework and hydrocarbon potential in the Yellow Sea. *Chinese Journal of Oceanology and Limnology* 26, 23-24.

Yi, S., Yi, S., Batten, D.J., Yun, H., Park, S.-J., 2003. Cretaceous and Cenozoic on-marine deposits of the Northern South Yellow Sea Basin, offshore western Korea: palynostratigraphy and palaeoenvironments. *Palaeogeography, Palaeoclimatology, Palaeoecology* 191, 15-44.

Zhang, Y., Wei, Z., Xu, W., Tao, R., Chen, R., 1989. The North Jiangsu-South Yellow Sea Basin. In: Zhu, X. (Ed.), *Chinese Sedimentary Basins: Sedimentary Basins of the World 1*. Elsevier, New York, pp. 107-123.

